GEORGIA INSTITUTE OF TECHNOLOGY OFFICE OF CONTRACT ADMINISTRATI

[x] ORIGINAL

[ ] REVISION NO. ___

PROJECT ADMINISTRATION DATA SHEET

Project No. B-552 DATE: June 3, 1981

Project Director: E. C. Burdette ~~School~~/Lab ECSL/BRD

Sponsor: Biomedical Research Support Grant (G-32-608)

Type Agreement: DHEW/PHS/NIH Grant No. 507-RR07024-16

Award Period: From 6/1/81 To 3/31/82 (Performance) 4/30/82 (Report

Sponsor Amount: $4,998 Contracted through

Cost Sharing: N/A ~~GTRI~~/GIT

Title: Microwave Imaging of Biological Targets

ADMINISTRATIVE DATA OCA CONTACT Faith G. Costello

1) Sponsor Technical Contact: -SEE BELOW-

2) Sponsor Admin./Contractual Contact: (Internal)
Dr. John W. Crenshaw, Jr., Biomedical Research Support Grant, School of Biology,
Campus

Reports: See "Comments" Below Security Classification: N/A

Defense Priority Rating: N/A

RESTRICTIONS

See Attached ___ Supplemental Information Sheet for Additional Require

Travel: Foreign travel must have prior approval - Contact OCA in each case. Domestic travel requires sponsor approval where total will exceed greater of $500 or 125% of approved proposal budget category.

Equipment: Title vests with N/A

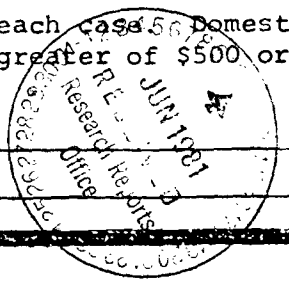

COMMENTS: Subproject under G-32-608
Reporting Schedule: (Internal only) Summary Report due by April 30, 1982.

COPIES TO:

Administrative Coordinator
Research Property Management
Accounting Office
Procurement Office

Research Security Services
~~Reports~~ Coordinator (OCA)
Legal Services (OCA)
Library, Technical Reports

EES Research Public Relat
Project File (OCA)
Other: Bio

GEORGIA INSTITUTE OF TECHNOLOGY OFFICE OF CONTRACT ADMINISTRATION

SPONSORED PROJECT TERMINATION SHEET

Date 9/10/82

Project Title: Microwave Imaging of Biological Targets

Sub Project No: B-552
(under Main Project No. G-32-608/Tornabene)

Project Director: E. C. Burdette

Sponsor: DHHS/PHS/NIH; Biomedical Research Support Grant (16th year)

Effective Termination Date: 3/31/82

Clearance of Accounting Charges: 3/31/82

Grant/Contract Closeout Actions Remaining:

NONE

- ☐ Final Invoice and Closing Documents
- ☐ Final Fiscal Report
- ☐ Final Report of Inventions
- ☐ Govt. Property Inventory & Related Certificate
- ☐ Classified Material Certificate
- ☐ Other _____

Subproject under G-32-608

Assigned to: ECSL/BRD (~~School~~/Laboratory)

COPIES TO:

Administrative Coordinator	Research Security Services	EES Public Relations (2)
Research Property Management	~~Reports Coordinator~~ (OCA)	Computer Input
Accounting	Legal Services (OCA)	Project File
Procurement/EES Supply Services	Library	Other GTRI

FORM OCA 10:78]

FINAL TECHNICAL REPORT
PROJECT B–552

MICROWAVE IMAGING OF BIOLOGICAL TARGETS: A FEASIBILITY STUDY

By

Everette C. Burdette

July 1982

Prepared for

BIOMEDICAL RESEARCH SUPPORT GRANT COMMITTEE
GEORGIA INSTITUTE OF TECHNOLOGY
ATLANTA, GEORGIA 30332

Under

NIH BRSG No. 507–RR07024–16

Submitted by

BIOMEDICAL RESEARCH DIVISION
ELECTRONICS AND COMPUTER SYSTEMS LABORATORY

GEORGIA INSTITUTE OF TECHNOLOGY

A Unit of the University System of Georgia
Engineering Experiment Station
Atlanta, Georgia 30332

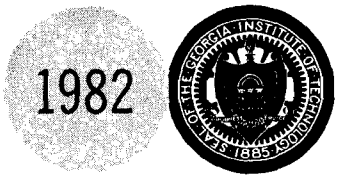

FINAL TECHNICAL REPORT

PROJECT B-552

MICROWAVE IMAGING OF BIOLOGICAL TARGETS: A FEASIBILITY STUDY

By

Everette C. Burdette

July 1982

Prepared for

BIOMEDICAL RESEARCH SUPPORT GRANT COMMITTEE
Georgia Institute of Technology
Atlanta, Georgia 30332

Prepared by

BIOMEDICAL RESEARCH DIVISION
Electronics and Computer Systems Laboratory
Engineering Experiment Station
Georgia Institute of Technology
Atlanta, Georgia 30332

FOREWORD

This report was prepared by personnel of the Electronics and Computer Systems Laboratory of the Engineering Experiment Station at the Georgia Institute of Technology. The work described herein was performed under National Institutes of Health, Biomedical Research Support Grant No. 507-RR07024-16 (designated as Georgia Tech Project B-552) during the period 1 June 1981 - 31 May 1982 and National Cancer Institute Grant No. CA22771 during the period 1 September 1980 - 28 February 1981. The described work was conducted under the general supervision of Mr. F. L. Cain, Director, Electronics and Computer Systems Laboratory, and Mr. J. C. Toler, Chief, Biomedical Research Division. It summarizes the objectives, activities, and results of a pilot study directed to determining the feasibility of using microwave imaging techniques as a means for non-invasive interrogation of biological systems. The author would specifically like to thank Mr. Harold Franch for his technical contributions to this effort.

Respectfully submitted,

[redacted]

E. C. Burdette
Project Director

APPROVED:

[redacted]

J. C. Toler, Chief
Biomedical Research Division

ABSTRACT

The overall objective of this research was to investigate microwave imaging techniques as a means for non-invasive interrogation of biological systems. Images which may be formed using non-ionizing electromagnetic radiation in the frequency domain differ from ultrasound and conventional X-ray images in that the characteristics determining the display are tissue dielectric properties and geometry, rather than density. Images of this type offer the possibility of assessing the functional state of anatomical structures because of the physiological relevance of dielectric properties. Known differences in dielectric properties of normal and diseased tissue may make possible the detection and quantification of pathological conditions such as atherosclerotic and malignant lesions.

The specific aims of this research effort included (1) a brief review of the existing relevant knowledge in the open literature, (2) examination of a few possible approaches for electromagnetic imaging, (3) design of a small prototype scanner system and antennas, (4) limited experimental testing in-vitro using phantom models whose dielectric characteristics mimic those of tissues of interest (e.g., muscle), and (5) initial development of software for more sophisticated processing of measured data. Specific aims (1), (3), and (5) were performed under a Biomedical Research Support Grant (Project B-552).

Feasibility studies confirmed that electromagnetic imaging of dielectric targets was dependent on multiple parameters including the relative difference in dielectric characteristics of the imaged structures, signal attenuation by the dielectric media, frequency of interrogation, dielectric discontinuities at the air/target interface, and type/degree of signal processing employed. With no data processing, it was possible to discriminate between two 3-mm diameter dielectric rods spaced greater than 4 mm apart embedded in a muscle-equivalent phantom 6 cm thick (frequency = 3 GHz).

TABLE OF CONTENTS

LIST OF FIGURES

LIST OF FIGURES

Continued

LIST OF TABLES

SECTION I
INTRODUCTION

With the recent public interest in harmful effects possible for X-radiation, there has emerged a wide recognition that alternative imaging techniques are needed. Alternatives currently being evaluated include ultrasonic imaging, zeugmatography, positron emission, and electromagnetic imaging. One alternative, imaging of tissues using signals in the microwave portion of the frequency spectrum, grew out of research in which passive microwave imaging was demonstrated to be of limited use in detecting certain breast cancers; however, it was recognized that active microwave imaging would be substantially more useful if rather complex technical problems could be solved. Research to solve these problems is now beginning [1-4]. Some of the medical applications of microwave imaging are (1) the diagnosis and management of respiratory and lung disorders, (2) the measurement of heart performance, (3) the early detection of arterial disease (the most common case of coronary heart attack and stroke), and (4) the detection of diseased tissue such as cancer.

An extremely important factor in the development of microwave imagery is the role played by the dielectric properties of the tissues under study. These properties are important because they determine the manner and extent to which tissues interact with an applied EM field. That is, phenomena such as (1) the phase delay and attenuation experienced by an EM wave propagating through tissue, (2) the coupling and/or reflection of incident EM energy with a biological system, and (3) absorption of EM energy by tissue are all determined by its dielectric properties. In cases where the dielectric properties of normal tissue and suspected lesions differ, the potential exists for detecting and imaging the lesion.

The serious medical problems posed by atherosclerosis, malignant lesions, and other diseases where angiographic and/or other similar diagnostic techniques are used illustrate the crucial need for instrumentation capable of detecting and quantifying such lesions. Ideally, this instrumentation would

- permit early detection of lesions,
- permit longitudinal and cross-sectional visualization of deep-lying vessels and/or organs via real-time image displays,

- o provide non-invasive detection and quantification techniques, and
- o leave no residue, cause no harmful side effects, and destroy no tissue.

To date, no instrumentation capable of satisfying all of these ideals exists. Instrumentation involving electronic X-ray image processing must be used in conjunction with intravenously-infused contrast agents; consequently, the X-ray approach is invasive with associated risks. Methods used to image neoplastic lesions, e.g. Computerized Axial Tomography (CAT), are primarily based on the use of ionizing radiation techniques and, although IR thermography and radiometric techniques have been used as diagnostic aids, an effective non-ionizing diagnostic imaging technique is yet to be developed. CAT is useful in the diagnosis of malignancies, but has typically not been used in the cardiovascular system because of problems associated with movement and the need for use of infused contrast agents. Feasibility studies have been conducted to determine whether instrumentation capable of measuring the magnetic moment of atomic nuclei could be useful in detecting and quantifying atherosclerotic lesions. With the current state-of-the-art, this technique, known as zeugmatography, does not appear feasible for detecting and quantifying lesions in deep-lying vessels. The instrumentation that presently appears most feasible for use in detecting atherosclerotic lesions is the ultrasonic B-scan system. Using this type system, lesions in vessels lying near the surface (such as the common carotid artery) can be resolved and imaged; however, for deeper-lying vessels (such as the iliofemoral, renal, and coronary arteries), the image resolution is not adequate. Nuclear magnetic resonance (NMR) is an old chemical analysis technique which has recently been applied to imaging of biological structures. The new techniques being developed show great promise for imaging some pathologies which are not well-suited for CAT diagnosis. However, extremely large electromagnets are required, present NMR systems are very expensive, and considerable research with regard to image interpretation is still needed.

A. Significance

The development of a non-invasive imaging technique based on the use of non-ionizing EM energy offers the unique potential for both imaging anatomical structures and assessing functional status. This unique potential exists

because of the biological relevance of complex permittivity (dielectric properties) to physiological function. The work performed under this pilot study indicated further that the detection of internal structures having largely different dielectric properties in lossy dielectric targets is indeed possible even with only minimal data processing. With further development, detection and imaging of dielectric anomalies in biological targets should be achieveable.

B. Research Objectives

The overall objectives of this research effort were to experimentally evaluate the feasibility of using microwave imaging techniques as a means for non-invasive interrogation of biological systems and to identify parameters which affect the achieveable resolution and penetration. Specific attention was given to the design of a small prototype electromechanical scanner system, and to limited experimental evaluation of feasibility using tissue-equivalent phantom models. In addition, various possible approaches for electromagnetic imaging were identified and development of data processing software was initiated. Work performed under National Cancer Institute (NCI) support is reported in Sections III and VI. Work supported by the Biomedical Research Support Grant is reported in Sections IV, V, and the final figure in Section VI.

SECTION II

BACKGROUND INFORMATION

The use of EM techniques in medical diagnosis dates back approximately one-half century when documentation was first published describing the measurement of electrical resistance across the lung as a means of determining the status of plumonary edema [5]. A decade later, EM techniques were introduced for monitoring blood flow [6,7]. This application has been highly successful, and the electromagnetic flowmeter is perhaps the most widely known EM device in medical diagnosis. Between 1940 and 1970 few, if any, successful diagnostic applications of EM techniques were introduced. Then, in 1971 [8], radiometric techniques in the microwave portion of the frequency spectrum were presented for diagnostic applications. These techniques were based on the fact that all bodies above absolute zero temperature emit energy in the form of EM radiation. By monitoring that portion of the radiation occurring in the microwave region, it was possible to detect structures at deeper locations within the body. Since 1971, a number of potentially significant diagnostic applications of EM techniques have been presented. These include

- the use of microwave energy in the management of lung disease [9],
- noninvasive microwave methods for measuring water content in lungs [10],
- a microwave Doppler radar for measuring arterial wall movement [11],
- noninvasive microwave techniques for measuring respiration [12], and
- a microwave stethoscope for measuring heart dynamics [13].

The possibility of using microwave techniques to image deep-lying structures in the body is an outgrowth of research knowledge gained from research in the above EM techniques for diagnosis and from the development of ultrasonic imagery and microwave radiometers. The potential for microwave imaging of biological structures has not been realized because of the existence of problems whose solutions appeared to oppose each other. These problems included (1) spatial resolution and signal loss, (2) dielectric discontinuities at the air/biological tissue interface, and (3) multipath propagation. Each of these problems stems from the fact that biological bodies are hetero-

geneous water-dominated dielectrics. Therefore, in the case of spatial resolution and signal loss, microwave frequencies at which the best spatial resolution could be obtained are unusable because of attenuation experienced by the signal as it propagates through the tissues. If lower frequencies are used to alleviate the attenuation, the longer wavelengths increase the illuminator aperture size required for efficient coupling of energy. In the case of near-field illumination (where resolution is largely a function of aperture size), as the aperture size is increased, the spatial resolution is correspondingly decreased. The dielectric discontinuity at the air/biological tissue interface causes a large portion of the incident EM wave to be reflected. This reflected wave is obviously of no benefit in imaging structures within the biological system. The multipath problem exists because, as EM waves propagate through tissues with different dielectric properties, they experience reflection and path bending; consequently, efforts to measure transmission loss and phase shift are compromised.

Recent studies have now resulted in at least partial solutions to the problems hindering the development of microwave imaging. Recent development of a needle-like probe-based system has made possible the characterization of the dielectric properties of different tissues (muscle, fat, skin, brain, bone, blood, etc.) in living animals [14-17]. The measurement system is based on an antenna modeling theorem that relates the complex reflection coefficient of an antenna in free space to the medium into which the antenna is radiating. The measured change in complex reflection coefficient, and therefore terminal impedance, is used in a computer program to compute the dielectric properties (relative to free space) of the biological material. Instrumentation used with the measurement probe consists of a reflectometer and a microcomputer-controlled network analyzer system for monitoring the complex reflection coefficient and computing the dielectric properties of the biological materials. The "in-vivo probe" measurement technique has been developed to the point that dielectric property measurements in living systems are routinely made on a swept frequency basis from 10 MHz to 10 GHz [15]. The significance of data resulting from these measurements lies in the fact that it is now possible to define, on an a priori basis, the absorption of EM energy by tissues of different dielectric properties. These properties play a key role in EM imaging, because the ability to image internal structures is dependent upon differing dielectric properties.

The in-situ dielectric characteristics of normal and diseased tissues have been measured [18-20] and recently, dielectric parameters have been related to physiological conditions [21-23]. Specific differences or changes in in-situ dielectric properties within a single tissue type or among tissues are reflective of the ability of EM imaging methods to discern the existence of pathophysiological conditions.

Jacobi et al. [24] have described transmit and receive antennas which were successfully operated at S-band frequencies while completely submerged in water. The water appears as semi-infinite space, and from a microwave imaging point of view, this substantially reduces measurement problems. For example, frequency and spatial resolution are inversely related. In the case of microwave near-field imagery, resolution can be considered in terms of the physical aperture of the transmitting and receiving antennas. When operating in the near field of an antenna, the spatial resolution of the imaging system monotonically improves with decreases in aperture size. The relative permittivity of pure water at 3 GHz is approximately 76; therefore, the velocity of propagation and wavelength are reduced by the square root of the relative permittivity, or 8.9. With this reduction in wavelength, the physical area of an open-ended waveguide antenna required to match the intrinsic impedance of the medium over a broad bandwidth is reduced by a factor of 76. Thus, by operating the transmitting and receiving antennas completely submerged in and filled with water, it is possible to achieve significant improvement in spatial resolution of the interrogating system for near-field imagery [1,2]. Also, the water essentially eliminates the multipath problems due to reflections from a non-anechoic environment. Finally, there is an improvement in energy coupling into the biological tissue because the dielectric properties of water are much more closely matched to tissue than are those of air.

A microwave system at 3.9 GHz has been assembled by Larsen and Jacobi and used to image phantom targets and isolated canine kidneys [3]. By immersing the antennas and scatterer in water, an improvement in spatial resolution by a factor of 8.9 was achieved [24] and problems with multipath caused by reflection were nearly non-existent. Using this approach, it was possible to achieve significant improvement in spatial resolution of the interrogating system for near-field imagery [1,2]. The system included electromechanical scanning and computer-aided image processing techniques. Evaluation of

this system concluded that magnitude and phase data were sufficient to reveal information relatable to the structural organization within canine kidneys. Regions corresponding to filtration were separable from regions corresponding to osmotic concentration, and both were easily separable from the pelvis. Subsequent efforts were directed toward improved performance by reducing undesired multipath propagation effects [4]. Water-immersed antennas were again used, but modulation of the interrogating signal used to measure attenuation and phase shift was "chirped." This means that the transmitted signal had a constant amplitude but varied in frequency with time in a linear fashion. This technique, designated "microwave time delay spectroscopy," allowed selective analysis of time delay and attenuation of the direct path that connects the transmitting and receiving antennas; thus, image contamination due to multipath propagation was reduced. Using this approach, Jacobi and Larsen were able to image objects as small as 6 millimeters in diameter and spaced 10 millimeters apart.

An inherent limitation to conventional resolution of microwave imaging systems is imposed by diffraction. Jacobi et al. [24] found that by immersing the antennas and scatterers in water and working in the near field, a practical resolution of 5 to 10 mm was attainable. This is consistent with the frequency used (3.9 GHz), the wavelength in water (11 mm), and the minimum aperture of the receiving antenna.

In some instances it is possible to achieve subwavelength resolution if an array of sources with a known radiation pattern is used and phase information for the scattered radiation is available. This method involves an inverse scattering approach which, although in general leads to nonunique solutions, may be pragmatically implemented using constraints available from some prior knowledge of the scattering object [25-27].

SECTION III

EXAMINATION OF VARIOUS APPROACHES FOR MICROWAVE IMAGING

Several approaches exist for microwave imaging of biological targets. Three likely approaches were examined: radiometric imaging, scattering parameter imaging, and time delay spectroscopic imaging. A review of a majority of the available literature concerning each of these three approaches was conducted. Radiometric imaging, as it has been employed to date, appears to be the least-likely candidate of the three approaches studied. The majority of the reported work deals with the detection of diseased tissue at various depths from a few millimeters (mm) to a few centimeters (cm) beneath the skin's surface [28-33]. Millimeter-wave radiometers offer potentially high resolution (~1 mm) and they have been used to obtain two-dimensional thermographic images of the female breast, re: mammography [33]. However, the useful penetration is at most only 1 or 2 millimeters. Detection of diseased tissue at greater depths results from the thermal conduction of heat from the diseased tissue (which is usually at a different temperature than its surrounding tissues) to the skin layers above. The state-of-the-art for millimeter-wave radiometer sensitivity is approximately $0.08^{o}K$ with careful engineering design. The minimum detectable tissue temperature differential at a depth of only 3 mm below the skin's surface is $0.5^{o}C$; this results in a surface radiometric contrast temperature of only $0.13^{o}C$ at a frequency of 35 GHz. This contrast temperature is just discernable by a state-of-the-art millimeter-wave radiometer ($0.08^{o}K$). However, the computation used to obtain the above contrast temperature assumes perfect dielectric coupling between the radiometer's antenna and the skin, which is usually not the case. Therefore, because of the extremely marginal sensitivity, coupled with the facts that any temperature difference between a lesion and surrounding tissues is likely to be small and that it is desirable to image tissues that are several cm deep, millimeter-wave radiometric imaging should not be considered for imaging deep-seated tissues or vessels. Microwave radiometry has also been used for breast cancer detection, with much of the work being done by Barrett and Myers [29-32]. Usable penetration depths can be obtained at microwave frequencies. However, no high-resolution near-field antennas have been used with their microwave radiometers. The smallest

antenna reported in use by Barrett and Myers [32] was a dielectric-loaded hand-held waveguide having approximate aperture dimensions of 1.27 cm x 0.63 cm. However, even if improved antennas were used, the major limitations would be the absolute sensitivity of the radiometer itself. Again, as in the case of millimeter-wave radiometric imaging, the resultant contrast temperature produced by a deep-seated lesion would just be too small to detect.

Active microwave imaging approaches appear to be generally the most attractive for achieving the goal of biological target imaging. In scattering parameter imaging, the energy transmitted through and reflected by the body is measured and this information is used to reconstruct an image of the target based on the electrical property composition. In the time delay approach, the microwave signal source is linearly "swept" in frequency over a range great enough to ensure unambiguous range resolution for biologically relevant path lengths. These methods provide similar information concerning the imaging of energy transmitted through (or reflected by) structures within the body, with an important difference. Scattering parameter imagery requires only single frequency radiation. The method is described more fully in Reference 3. The advantage of the time delay spectroscopic imaging technique over scattering parameter transmission measurements is that the time delay method does not suffer from multipath propagation (arrival of transmitted energy at the receiving antenna via two or more propagation paths). Otherwise, the two methods (scattering parameter and time delay) are identical in that both transmission and reflection measurements may be made. Multipath propagation causes serious problems with respect to determination of the image reconstruction path because it cannot be assumed that the energy measured by the receiving antenna followed a single path. This problem has also been identified by others involved with the use of microwave diagnostic techniques [34]. The time delay spectroscopic approach for microwave imaging effectively eliminates image reconstruction problems due to multipath. Time domain measurements of a target's response to pulsed-wave interrogation can also be utilized to circumvent the multipath problem. However, bandwidth requirements of the receiving instrumentation and the very fast rise-time needed for the transmitted pulse dictate the use of very complex and expensive instrumentation. The limited swept frequency (time delay) approach described by Jacobi and Larsen [4] is easier to implement and they claim that excellent range resolution is obtained.

A. Role of Dielectric Properties in Microwave Imaging

At microwave frequencies (0.3 - 30 GHz), the propagation constant which defines the attenuation and phase shift of an EM wave is determined by the complex permeability and permittivity of the tissue through which the wave propagates. The permeability relates to the magnetic properties of a material. For most biological materials, the magnetic permeability is equal to that of free space and magnetic losses are nonexistent; thus, permeability is not an influencing factor in a biological microwave image. The complex permittivity of tissue at microwave frequencies is determined primarily by its water and electrolyte content and by its temperature. Tissue proteins also influence the permittivity (particularly at the lower microwave frequencies), although to a lesser degree. The complex permittivity, $\varepsilon^* = \varepsilon' - j\varepsilon''$ consists of real and imaginary parts. The real part, ε', is conventionally expressed relative to the permittivity of free space by the ratio $\varepsilon'/\varepsilon_o$, which is the relative dielectric constant, expressed as K'. The imaginary part, ε'', of the complex permittivity is called the loss factor, which is expressed relative to free space permittivity as $K'' = \varepsilon''/\varepsilon_o$. The loss tangent is simply the ratio $\frac{\varepsilon''}{\varepsilon'} = \tan\delta$. The electrical conductivity σ is just $\omega\varepsilon'$, where $\omega = 2\pi f$ is the angular frequency and f represents the frequency in hertz of the EM field. The above quantities are collectively known as the dielectric properties of a material.

It has been well documented [35] that tissues differ in their dielectric properties at microwave frequencies and more recently, results of <u>in-situ</u> measurements of living tissues compared to measurement results from excised samples of the same tissue types indicate the existence of differences in their dielectric properties, particularly for fat, brain, and renal tissue [14]. Recent work performed in our laboratory [18-20] and by others [36,37] has shown that changes in dielectric properties are indicative of physiological changes which may be of diagnostic significance. Under NCI support, we have determined the existence of significance differences in the <u>in-vivo</u> dielectric properties of malignant tumors and normal host tissues [21-23]. Accurate <u>in-vivo</u> dielectric property information is necessary for the successful application of non-ionizing electromagnetic diagnostic techniques in medicine, particularly with respect to imaging and other diagnostic applications (measuring physiological changes, differentiating between normal and diseased tissues, or elucidating pharmaco-physiological effects due to drugs).

Tissue dielectric properties are of key importance to microwave imaging because the ability to relate physiological or pathophysiological alterations to changes in tissue dielectric properties (within a fixed geometry) is effectively a measure of the ability of microwave imaging methods to discern the existence of pathological conditions in the intact tissue, organ, or organism. In quantitating atherosclerotic lesions, the differences in the properties of normal arterial constituents and calcified deposits, together with their respective morphologies (advanced plaques, ulcerated lesions, total occulsion, etc), would be reflected in their microwave image. Differences in the dielectric properties of normal and malignant tissue also make microwave imaging of neoplasms (especially breast cancer) a realizable possibility [21]. The existence of tissue dielectric property differences and the dependence of scattered microwave energy upon target composition and geometry, suggest the possibility of forming a microwave image of biological targets [9]. Yet, as discussed in Section II, only recently have imaging results been published based on microwave illumination of dielectric targets within a surrounding medium predominantly composed of water [1,2].

Tissue/electromagnetic field interaction is dominated by static and dynamic electrical properties (ohmic loses due to ionic conductivity and dielectric losses due to polar molecules) which depend largely upon water content. As mentioned previously, protein content also exhibits a minor influence, with changes in conformation and stereospecificity manifested as small changes in electrical properties [38]. Swept-frequency or time-domain microwave imaging for dispersion analysis offers a potential means for determining the state of the water present. Such multifrequency measurements may be useful to distinguish between hydration water, solvent water, and free water as physiologically important entities. Further, a careful selection of interrogation frequencies can be used to maximize the sensitivity of the imaging method to discern small dielectric changes in the broad δ-dispersion region [39] which are due to a dielectric dispersion of protein-bound water and partial rotation of polar subgroups.

Attenuation of an EM wave in the target material is a function of several parameters (frequency, dielectric constant, conductivity). For a given frequency, the wavelength is smaller in materials of higher permittivity, ϵ^*, and/or permeability, μ^*, since: $\lambda = \frac{1}{\sqrt{\mu^*\epsilon^*}}$. The frequency (and thus λ) used for interrogation is in turn limited by attenuation of the incident signal power, P_o, upon passing through the target. The attenuation constant,

α (in nepers per meter), is related to the angular frequency, ω, and to the conductivity (σ) of the material as follows [40]:

$$\alpha = \omega \sqrt{(\mu^*\varepsilon^*/z)} \left[\sqrt{1+ \left(\frac{\alpha}{\omega\varepsilon}\right)^2} -1 \right] . \qquad (1)$$

Since water has a dispersion of 20 GHz, the term $\frac{\sigma}{\omega}$ reaches a peak at that frequency. This dispersion is responsible in part for the rapid increase in attenuation with increasing frequency (decreasing wavelength). As frequency is increased, the attenuation of high-water-content biological materials increases at a very rapid (non-linear) rate. For the illustrative simple case of a plane wave traveling in the z-direction, the relationship between the power at point z, $P_t(z)$, and the incident power is:

$$\frac{P_t(z)}{P_o} = e^{-2\alpha z} . \qquad (2)$$

Table I illustrates the attenuation through 15 centimeters of water at 298^{o}K for a variety of frequencies based on the Debye dispersion relationship [41]. From this table, it is clear that frequencies above 5 GHz are impractical for imaging even in distilled water if power levels are restricted to approximately 1 milliwatt.

The minimum required incident power level for transmission scattering parameter measurements is dependent upon signal attenuation through the dielectric medium (or media) at the operating frequency and upon the noise floor of the receiving system. Phase/amplitude receivers are presently available which have a noise floor of -120 dBm, a 100-dB dynamic range, and a 6 dB noise figure. Receiving system performance can be further improved through the addition of a low noise preamplifier. Adding a preamplifier with 30 dB gain having a 1.5 dB noise figure improves the overall noise figure and reduces the noise floor to below -150 dBm. For an operating frequency of 3 GHz, the attenuation through a 15-cm thick muscle-equivalent dielectric medium is approximately 125 dB. If a system signal to noise ratio of 20 dB is specified, the required incident power density would be 0.3 mW/cm^2, assuming a 1 cm^2 receiving aperture area. For less thick media and/or smaller signal to noise ratios, the incident power density may be reduced accordingly. A practical limit would likely be 10 dB signal to noise ratio, resulting in a minimum incident power density of 0.03 mW/cm^2

TABLE I

ATTENUATION THROUGH A 15 CM-THICK

SAMPLE OF DISTILLED WATER

(Hz) Frequency	K'	K"	(Nepers/m) α	ATTENUATION THROUGH 15-cm (dB)
10^8	78	0	0.0	0.0
5×10^8	78	1	0.6	0.8
10^9	76	6	7.2	9.4
5×10^9	72	15	92.1	120.0
10^{10}	56	31	419.4	546.0
5×10^{10}	24	31	2,889.3	3,761.9
10^{11}	8	18	5,068.6	6,600.0
5×10^{11}	3.8	7	15,122.1	19,689.0

for a 15-cm thick dielectric media. A limit on the maximum incident power density is dictated primarily by non-ionizing radiation hazard considerations. As a rule-of-thumb, the incident power density used should be at least an order of magnitude below the microwave oven leakage standard (5 mW/cm^2).

B. Parameter Tradeoffs

Numerous factors have contributed to the low number of successful efforts to obtain high-quality microwave images in aqueous dielectrics. These factors include frequency, choice of near-field versus far-field illumination, detection, antenna design, and non-linear propagation paths due to the spatial distribution of different tissue complex permittivities (electrical properties). Susskind [9] points out the conflict in selecting a suitable operating frequency: greater penetration requires a lower operating frequency, while to achieve greater resolution an operating frequency higher in the microwave (or even millimeter-wave) band is usually required. (Penetration deep into the thoracic cavity and/or abdomen requires a lower operating frequency; however, in diffraction-limited EM illumination schemes, improved resolution dictates the use of a higher operating frequency). This brings us to the next factor: near-field illumination versus far-field illumination. Under far-field illumination conditions, the total scattered field is utilized, but resolution is diffraction-limited and reflections at air-dielectric interfaces can adversely affect image quality and reduce sensitivity. Under near-field conditions, the major factor affecting resolution is aperture area which is again related to wavelength. As stated in Section II, recent research efforts in microwave imaging have been reported in which wavelength contraction was achieved by locating the antenna in an aqueous medium [1,2,24]. Thus, the effective aperture area of an open-ended waveguide or horn antenna designed for operation at 3 GHz in free space is increased by a factor of 76 when operating in pure water. Conversely, the required physical aperture area of an open-ended waveguide antenna that can be matched to the intrinsic impedance of the medium is reduced by the same factor. Thus, by operating the antennas in water or another high dielectric constant medium, a significant improvement in spatial resolution of the imaging system can be achieved.

Resolution also can be increased by increasing the operating frequency, thereby permitting a further reduction in the aperture size. However, transmission loss increases monotonically with frequency. In high water content

tissues, the transmission loss at 2 GHz can approach 500 dB per meter and at 6 GHz, the loss increases to more than 1000 dB per meter. Therefore, tradeoffs between resolution and signal attenuation (i.e., useful penetration) must be carefully evaluated in view of the in-vivo electrical properties of the interrogated tissues in order to achieve an optimum compromise.

By definition, resolution is the minimum detectable separation of scatterers. An inherent limit on resolution, as conventionally considered, is imposed by diffraction of the radiation. This limit is generally proportional to the wavelength. For example, using the Rayleigh criteria [42] for angular resolution of far-field images of self-luminous objects, θ_r is proportional to λ/d, where θ_r is the angular resolution, λ is the wavelength of the radiation, and d is the receiving aperture. This limit is determined by the overlap of the main diffraction peak of one scatterer with the first minimum of the diffraction pattern of the second.

Diffraction is a serious limitation in microwave imaging because of the long wavelength (typically mm to cm) as compared to that of x-rays or particle beams (typically angstroms). In these latter cases, resolution is generally limited by the number of rays taken and counting statistics. As discussed by Jacobi et al. [24], some improvement to the resolution of microwave imaging systems can be obtained by immersing the radiating source, object to be imaged, and receiver in a high dielectric medium where the wavelength is contracted by a factor of $\sqrt{K}$. An additional improvement may be obtained by working in the near field of the antennas where the resolution is limited by the effective aperture of the antennas used. Practically, the resolution is limited by the minimum usable detectable signal level of the receiver and by the transmission loss of the signal through the tissue at the penetration depth where interrogation is desired.

There is a possibility of attaining greater resolution. Under certain conditions, resolution of subwavelength objects is possible. This phenomena, referred to as superresolution [25], is possible in certain well defined situations where the scattering object is localized, multiple sources are used, and phase as well as magnitude measurements of the scattered field are available. An example of superresolution is the reconstruction of an array of dipole radiators from far field data [25]. In this case using some prior knowledge of the source, resolution is not diffraction-limited.

In the case of microwave imaging, it may be possible to obtain superresolution using an array of transmitters whose unperturbed radiation pattern is well defined and measuring phase and amplitude of the scattered field. Here the feature of relatively low frequencies is an advantage in that phase measurements are possible, whereas this information is generally not available for X-ray imaging.

In the preceding discussion relating to frequency selection, near-field versus far-field illumination, and resolution, important attributes of antenna design considerations are evident. Near-field illumination of the biological target offers potential advantages over far-field illumination as discussed above. A key antenna design consideration remaining is how to develop a system with a rapid scanning capability (possibly electronic, under computer control) and yet maintain the increased resolution obtainable using dielectric-loaded small apertures with maximal coupling to the biological medium. One feasibile solution to this problem would be to design a scanning system which is both electromechanical and electronic in nature, and with both operating under computer direction. In this design, an array of antennas each having a very small aperture area and loaded with a high dielectric constant material would be scanned electronically in one linear direction while simultaneously being mechanically scanned in an orthogonal direction. Mechanical scanning or "stepping" in the direction of the electronic scanner would necessarily be possible to permit "capturing" missed information due to array element spacing. One possible design of the antenna scanning system just described is shown diagrammatically in Figure 1. Such a system could utilize linearly polarized antennas from which data would be recorded for two orthogonal polarizations. These data would then be processed in a manner which yields the greatest amount of target information from the measured data. Another antenna-related factor of great importance to the sensitivity of microwave imaging methods in biological targets is the efficiency of energy coupling into the body. Optimally, the dielectric characteristics of the antenna loading material and the body would be nearly identical, and any intervening space necessarily would be filled with a similar dielectric medium. This would greatly reduce reflection at the surface of the body resulting in better coupling of energy to the body and improved efficiency of the interrogating system. Another benefit is related to the processing of signals reflected from internal interfaces, such as those we wish to

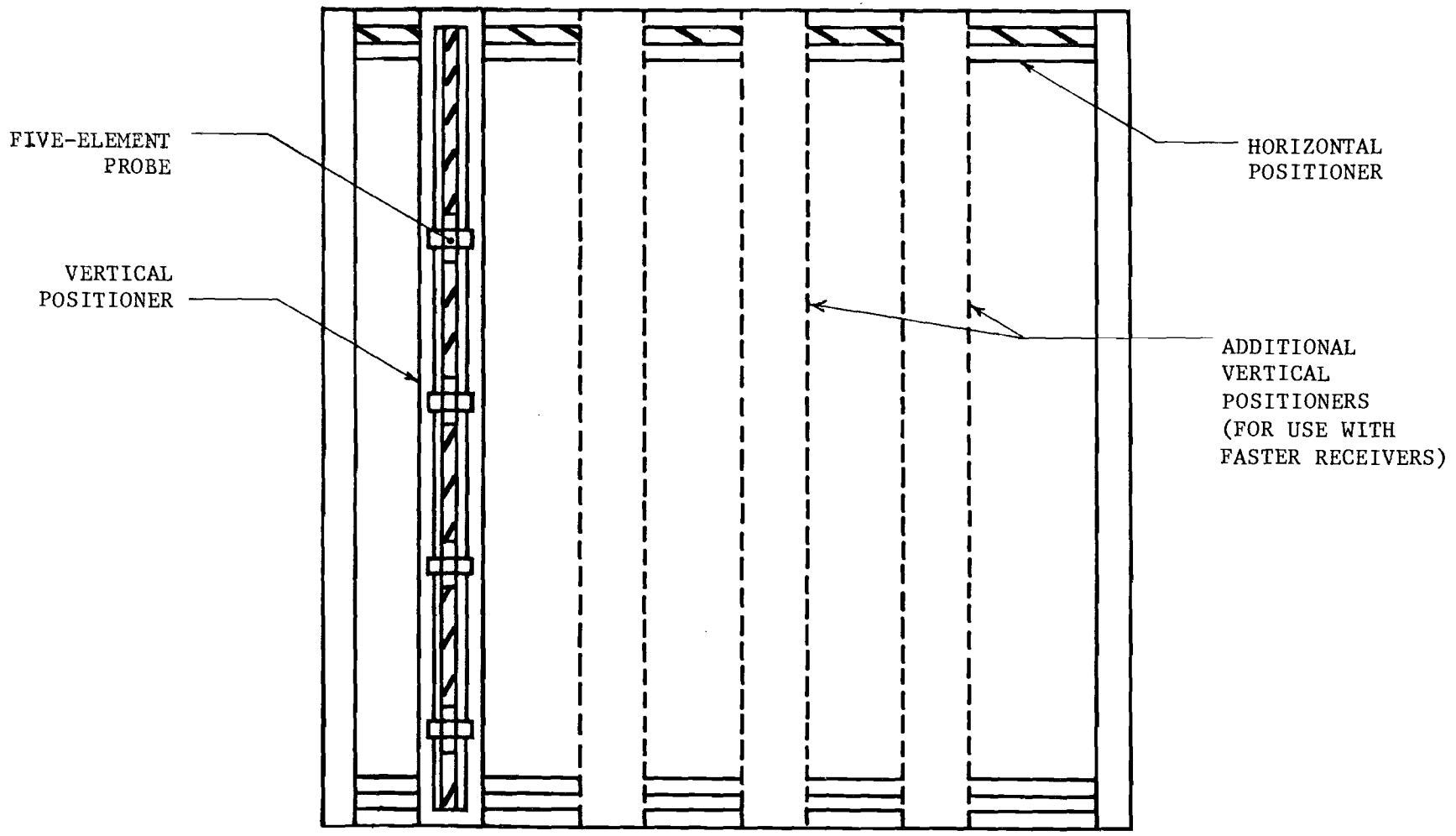

Figure 1. Conceptual drawing of electromechanical scanning array illustrating possible five element per probe configuration.

discern (fat deposits on arterial walls, tumors deep-seated in normal tissues). That is, the large reflection at the air - tissue interface which would be present if no dielectric coupling medium were used would impose a significantly greater dynamic range requirement and sensitivity requirement on the microwave receiving system (and could possibly require higher transmitted energy levels) in order to detect internal structures. Therefore, the coupling medium between the antenna and body should minimize, but not necessarily completely eliminate, the reflection at the body surface, because it is an important clinical reference point [24].

Another limitation of a microwave imaging system is related to the smallest size that a datum point can be made (basically the smallest interval between two successive interrogation points) and the accuracy of that interval. Larsen and Jacobi [3,4] used an electromechanical positioning device to move a pair of horn antennas over a grid to obtain image information. A somewhat similar mechanical positioner design was used in this research. When arrays are used, switching between antenna array elements can be accomplished using microwave PIN diodes. Scan times on the order of seconds are feasible. Rapid scan times are essential if microwave imaging is to be made practical for clinical use.

SECTION IV

ELECTROMECHANICAL SCANNER AND ANTENNA DESIGN

A. Scanner Design

Under this pilot study, a number of scanner configurations were examined. Electronic scanning systems were not considered because the considerable expense of developing an electronically-scanned array was well beyond the scope of this pilot study. Mechanical and electromechanical scanner configurations designed ran the gamut from a manually operated mechanical system to an automated electromechanical system using stepping motors and optical encoders. In every configuration considered, movement of the receiving and transmitting antennas in two dimensions over a planar surface was provided. The final design was a compromise between needed features for computer-controlled positioning/data acquisition and budget constraints. That design is illustrated in Figure 2.

Two antennas, one for transmitting and one for receiving, are mounted on vertical extensions of a horizontal cross bar which is attached to the Y-coordinate positioner. Positioning of the antennas over a 9.5-in. x 12-in. X-Y plane was accomplished by using two Unislide (Velmex, Inc., Bloomfield, NY) lead screw assemblies mounted orthogonal to each other (Figure 2). The Y-coordinate positioner (Unislide A2500 1/4-in. lead screw) mounts vertically and is controlled manually. The X-coordinate positioner (Unislide B-2515P20-J 1/4-in. lead screw) is motorized and mounts horizontally between two support blocks. Precision of the lead screw assemblies is 0.0015 inch. Movement in the X-direction is controlled by an external computer system (Hewlett Packard 5451C). The motor drive is activated and stopped by the computer system and a gear-train potentiometer assembly (revolution counter) provides x-position information to the computer. Data sampling by the computer was synchronized to the x-position information. The data acquisition and processing software are discussed in Section V of this report. Scanning in the X-Y plane is accomplished by manually setting the Y-position and automatically scanning in the X-direction under computer control. A new Y-position is set manually after each X-scan.

Larsen and Jacobi [1,3] reported that the resulting image quality from sampled scattered microwave fields is highly dependent upon positional accuracy

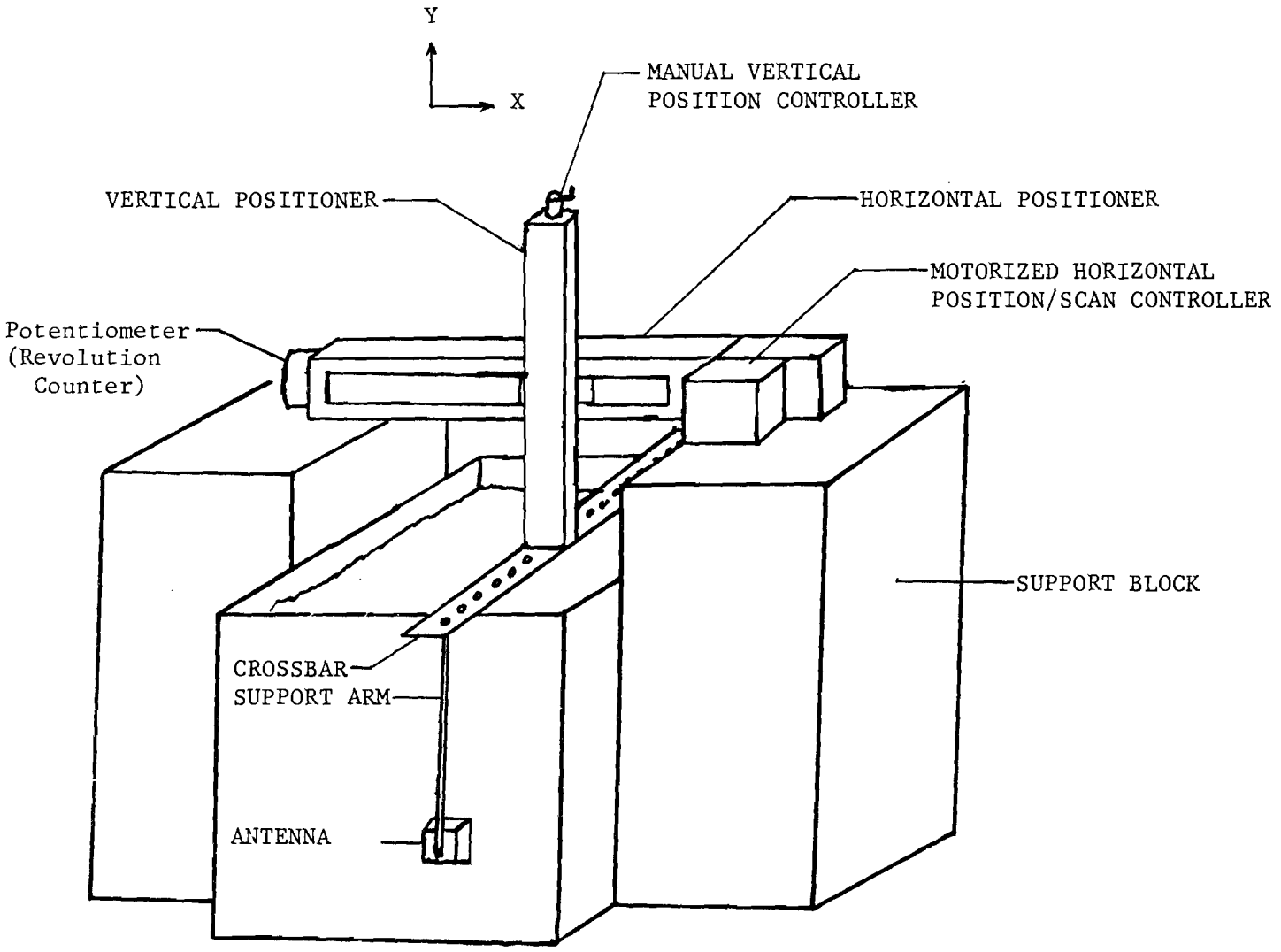

Figure 2. Illustration of electromagnetic/mechanical scanner system used for feasibility studies.

of the scanner system. For the scanner design of Figure 2, the positioned accuracy of the computer-sampled transmitted data is primarily dependent upon the following factors:

- o Precision of the Unislide lead screw assemblies;
- o Accuracy of the potentiometer assembly (revolution counter);
- o Computer data-point sampling time.

The dominant affector of accuracy in our system is the revolution counter, or potentiometer assembly. Most standard potentiometers have a linearity accuracy of 0.25%. Klinger and Litton manufacture potentiometers having linearity accuracies of 0.1% and 0.05%, respectively. However, the cost of these potentiometers is five times greater than the cost of a standard potentiometer (0.25% linearity). Thus, a Velmex Model 370 gear-train potentiometer was selected. The linear positional-readout accuracy is given by

$$\text{Position Inaccuracy} = (PC)N + 0.0013, \tag{3}$$

where PC is the potentiometer constant (= 0.0002 for Velmex potentiometer and = 0.00004 for Litton potentiometer), N is the gear turn ratio (N = 25), and the additive constant is the inaccuracy due to the lead-screw mounting. For the Velmex Model 370 potentiometer, the system repeatability (position inaccuracy) is $\pm$ 0.0063 in. (0.162 mm). The positional inaccuracy due to the computer sampling time for "fly-by" acquisition of data is $\pm$ 0.02 mm worst case. Thus, the total X-position inaccuracy is $\pm$ 0.182 mm. Larsen and Jacobi [1,3] reported that position inaccuracies greater than 0.25 mm significantly affected resultant image quality in their experiments. Use of the Litton potentiometer, instead of the standard Velmex unit used in this study, would decrease the overall positional inaccuracy by an additional factor of four or more.

B. Antenna Design

First, we will briefly examine antenna design factors relating to aperture size and resolution. In Section III of this report, the use of dielectric loading to decrease the physical aperture of an antenna operating at 3 GHz was described. The effect of aperture size on the resolution of a dielectric object located in the signal path between two antennas (one transmitting, one receiving) aligned on-axis facing each other was examined as a function

of aperture size. The experimental configuration and results are shown in Figure 3. The two waveguide aperture sizes are indicated in the figure. The near-field signal attenuation caused by the dielectric rod is much smaller, and the spatial pattern produced is much broader (less resolved) for the larger aperture, which has approximately a cosine distribution, than for the smaller aperture. The small-aperture antennas were loaded with a low loss, high dielectric constant material (tightly-packed T_iO_2) which permitted operation of the small antennas at the same frequency as the larger ones. The dielectric rod produced greater signal attenuation between the two small-aperture antennas than between the larger antennas due to the fact that the same diameter dielectric rod used in both cases blocked a significantly greater porition of the aperture of the small antenna. However, dielectric loading of the smaller-aperture antenna to permit operation at a lower frequency (by a factor equal to the square root of the relative dielectric constant of the loading material) than possible in air did decrease the antenna's efficiency. Thus, more signal or greater receiver sensitivity was required. Dielectric loading to reduce physical aperture area resulted in a significant improvement in resolution while permitting operation at frequencies low enough to provide adequate penetration of the signal for imaging deep-lying structures. Carried to an extreme, dielectric loading could be used to reduce aperture size to any degree desired. However, there exist practical limitations. These limitations include antenna efficiency, receiver sensitivity and noise figure, impedance mismatches between the tissue and the antenna, and transmission loss through tissue. However, antenna performance can be optimized by selecting the smallest possible aperture size and highest frequency which can be employed within the constraints of signal attenuation through lossy tissues (those with high water content) and state-of-the-art receiver design. Coupling efficiency between the antenna and the tissue can be maximized by impedance matching with dielectric materials of appropriate dielectric constant. Ideally, the dielectric characteristics of the antenna loading material and the body would be nearly identical (except for dielectric loss), and any intervening space necessarily would be filled with a similar dielectric.

In the feasibility studies conducted during this program, the intervening space between the transmitting and receiving antennas was filled with a muscle-equivalent phantom model. Thus, the impedance of the intervening

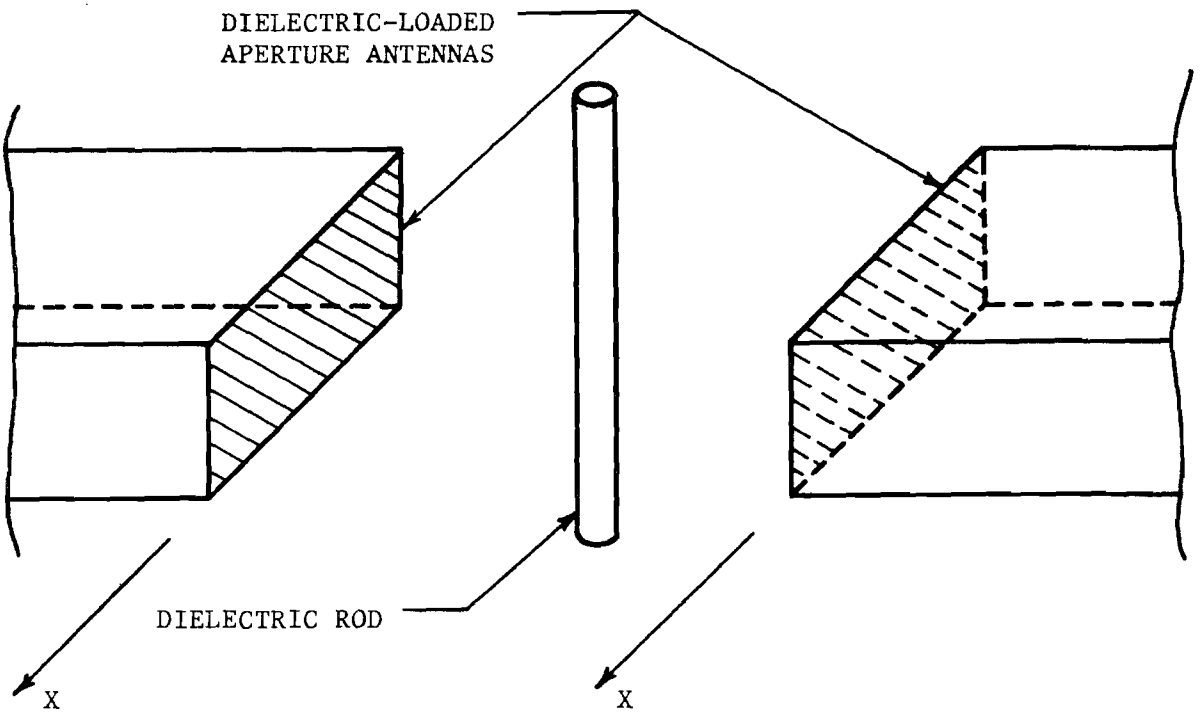

(a)

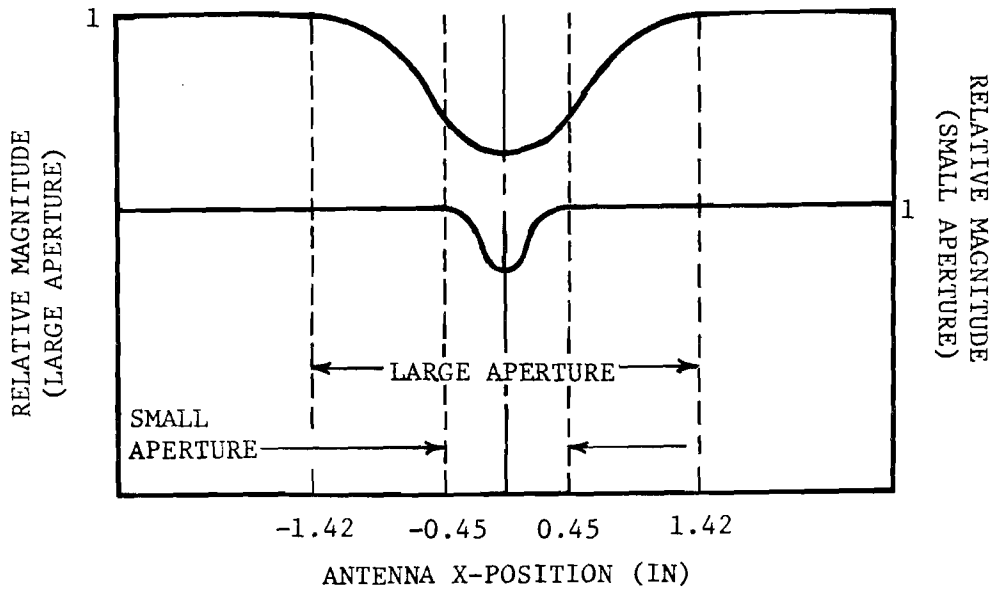

(b)

Figure 3. Feasibility studies on imaging a dielectric rod with two dielectric-loaded aperture antennas. (a) Experimental configuration. (b) Aperture size effect on resolution. The dielectric rod is centered at x = 0.

dielectric medium was similar to the impedance of the dielectric-loaded antenna.

SECTION V

DATA ACQUISITION AND PROCESSING SOFTWARE DEVELOPMENT

During this pilot study, computer algorithms for data acquisition were written and tested. Also, development of software for processing of measured scattering parameter data was initiated. All software was developed for use on a Hewlett Packard 5451C Fourier Analyzer system, which includes a HP1000 Series E minicomputer and 5 Mbyte disk.

A. Data Acquisition Program

The data acquisition program was specifically written for use with the semi-automatic electromechanical scanner system described in Section IV of this report. The program reads a voltage from the Velmex potentiometer assembly which is proportional to X-position. The computer samples amplitude and phase of the scattered field from the target as a function of potentiometer output voltage and thus, X-direction position. The program directs the system to automatically pull data points from the source on Channel A of the Fourier Analyzer based on a voltage on Channel B (potentiometer). The program pulls points from A when the voltage on B reaches the prescribed increments. It rejects anything that is not within $\pm$ 1% (this may be adjusted to the desired accuracy) of the desired point. It takes the nth data block (64 words currently) and pulls the center point and then puts that point in the nth position of another data block. When all the data from one scan have been acquired, the data are displayed and stored. A maximum of 6 data points per second can be acquired. If data are presented at a faster rate, the program stops and asks to be returned to the previous point. It reads 64 points in 10 seconds. Accuracy of the "fly-by" acquisition is currently $\pm$ 1%; it may be made more accurate by reducing the scanning rate. Data block size is 64 points. A block size of 128 is possible, but data acquisition time is doubled. Measured data are stored in a digitized data block on the disk. A flow chart of the data acquisition program is given in Figure 4.

B. Fourier Transform Program

This program performs a FFT (Fast Fourier Transform) on each line (each block) of a group of data (e.g., every block of a 64 point by 64 block image).

FLOW CHART DATA AQUISITION

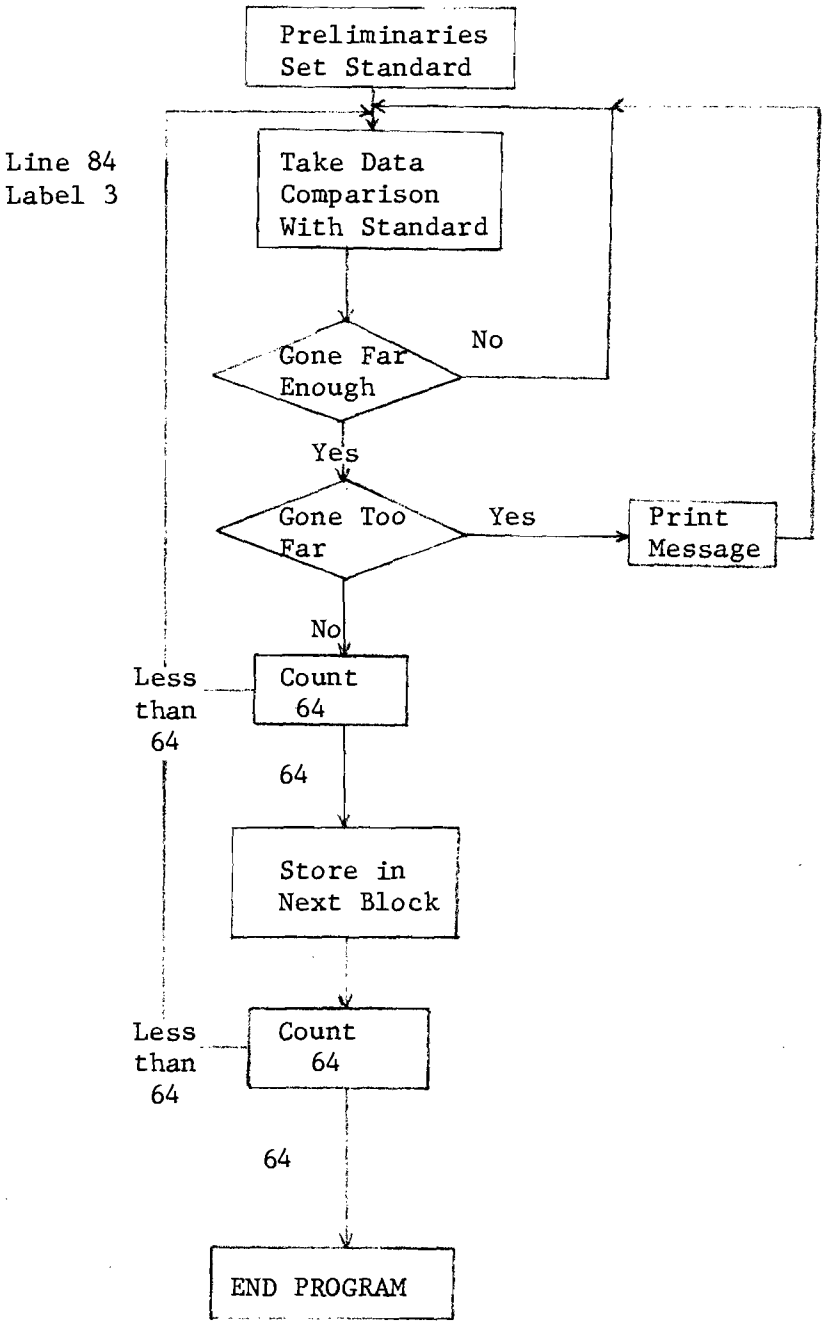

Figure 4. Flow Chart of Data Acquisition Program

The X-direction is the one in which 64 blocks are located. The program can switch data block orientation from the X to the Y direction. If another transform is run in the X direction after interchanging data block orientation, then it is really transforming in the Y-direction since the X and Y directions have been interchanged. Figure 5 is the flow chart for the Fourier transform program.

C. Bivariate Interpolation Program

Consider an integrand I of the form

$$I = \int_{v_1}^{v_2} \int_{u_1}^{u_2} f(u,v)\, e^{j(au+bv)} du dv \tag{4}$$

where the integration is performed on the square patch shown in Figure 6. If the function f(u,v) is defined at the corners of the patch, the function within the patch can be approximated by the 4-point bivariate interpolation formula [43]:

$$\begin{aligned} f(u_0 + pg,\, v_0 + qh) = {} & (1 - p)\,(1 - q) f_{00} + p(1 - q) f_{10} \\ & + q\,(1 - q) f_{01} + pq\, f_{11}, \end{aligned} \tag{5}$$

where,

$f_{00} = f(u_o, v_o)$,
$f_{01} = f(u_o, v_o + h)$,
$f_{10} = f(u_o + g, v_o)$, and
$f_{11} = f(u_o + g, v_o + h)$.

Thus, the integral I_i on the i'th patch takes the form,

$$I_i = \int_{q=0}^{1} \int_{p=0}^{1} f(p,q) e^{ja(u_o + pg)} e^{jb(v_o + qh)} [(gh) dp dq]\,. \tag{6}$$

Using the interpolation formula given in equation (5), this integral can be expressed as the sum of four integrals as

FLOW CHART FOURIER TRANSFORM

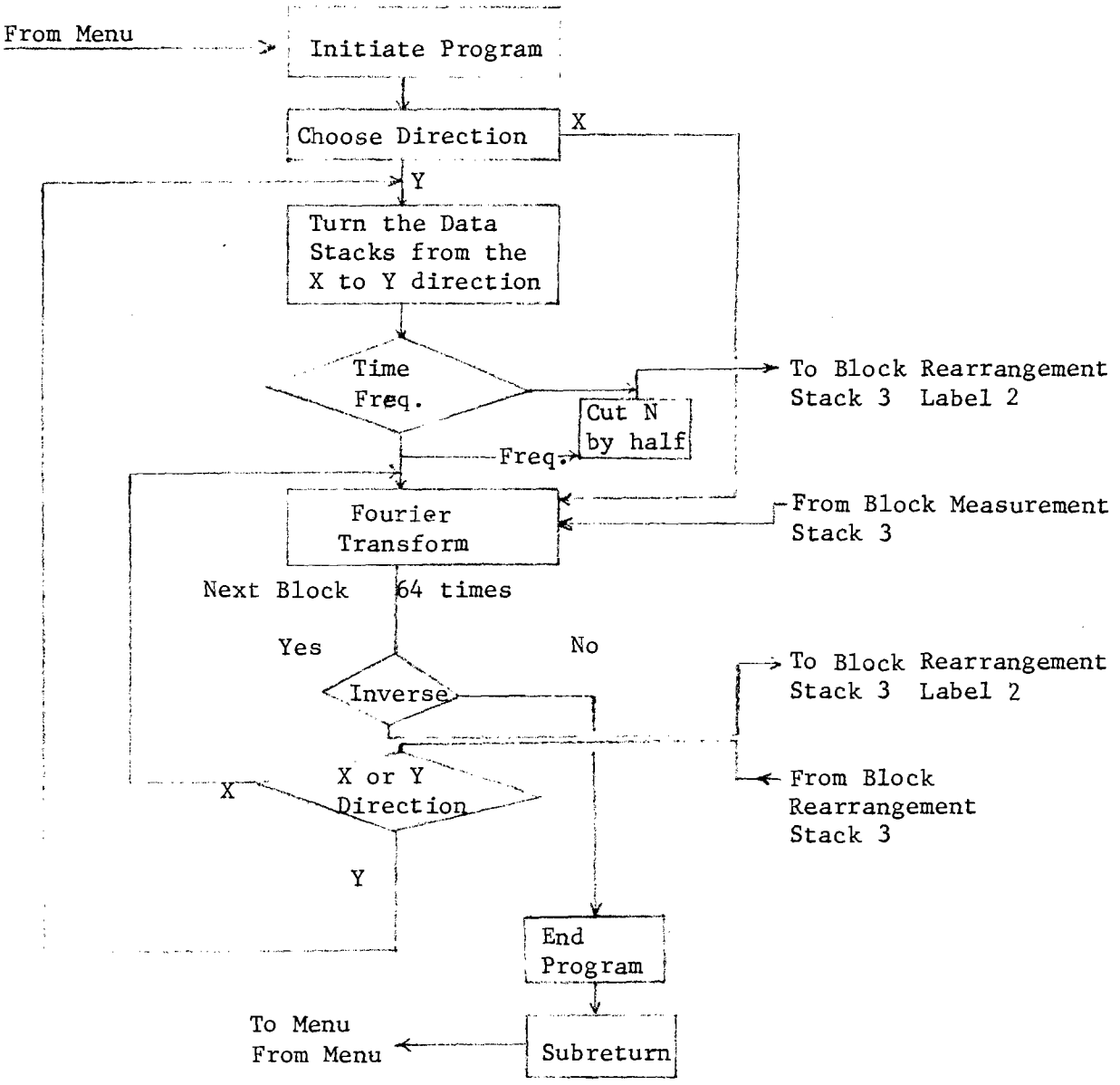

Figure 5. Flow chart of Fourier transform algorithm.

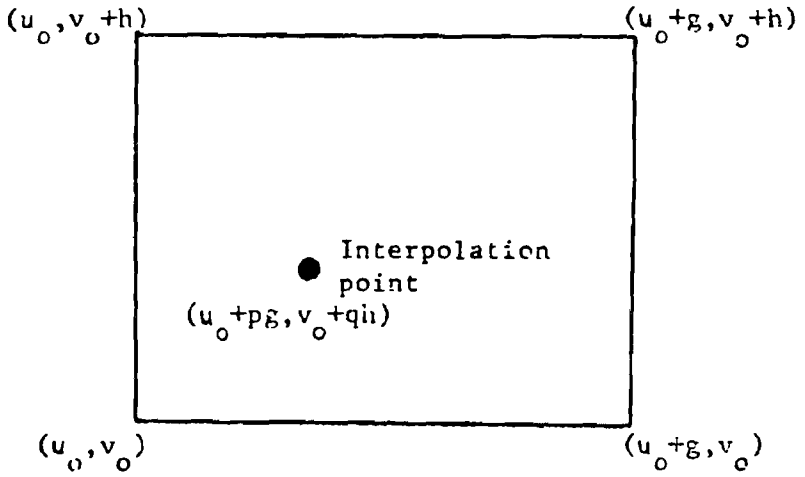

Figure 6. Geometry of the Surface Patch Used in the Bivariate Interpolation Integration Formula.

$$I_i = (gh)\, e^{j(au_o + bv_o)} \{ f_{00} I_{i,1} + (f_{10} - f_{00}) I_{i,2} + (f_{01} - f_{00}) I_{i,3} + (f_{00} - f_{01} - f_{10} + f_{11}) I_{i,4} \} , \tag{7}$$

where the integrals $I_{i,j}$ are given by

$$I_{i,1} = \int_{q=0}^{1} \int_{p=0}^{1} e^{jagp} e^{jbhq}\, dpdq ,$$

$$I_{i,2} = \int_{q=0}^{1} \int_{p=0}^{1} p\, e^{jagp} e^{jbhq}\, dpdq ,$$

$$I_{i,3} = \int_{q=0}^{1} \int_{p=0}^{1} q\, e^{jagp} e^{jbhq}\, dpdq , \quad \text{and}$$

$$I_{i,4} = \int_{q=0}^{1} \int_{p=0}^{1} p\, q\, e^{jagp} e^{jbhq}\, dpdq .$$

These integrals are evaluated in closed form as

$$I_{i,1} = [\frac{1}{jag} (e^{jag} - 1)][\frac{1}{jbh} (e^{jbh} - 1)] ,$$

$$I_{i,2} = - \frac{1}{(ag)^2} [e^{jag}(jag - 1) + 1][\frac{1}{jbh} (e^{jbh} - 1)] , \tag{8}$$

$$I_{i,3} = - \frac{1}{(bh)^2} [e^{jbh} (jbh - 1) + 1][\frac{1}{jag} (e^{jag} - 1)], \text{ and}$$

$$I_{i,4} = \frac{1}{(ag)^2 \cdot (bh)^2} [e^{jag}(jag - 1) + 1][e^{jbh}(jbh - 1) + 1] .$$

These closed form expressions were implemented in a computer algorithm and are a two-dimensional form of the linear Filon Quadrature formula [43].

When these formulas are used to evaluate a given integrand f(u,v), the patch size must be chosen such that the bivariate interpolation formula gives a good approximation to the function over the integration patch. An integration over a large area can then be performed by using a grid of patches which covers the entire integration area. Formulas of this type have been found to be more accurate than the trapezoidal integration rule for the evaluation of radiation integrals.

D. Data Filtering Programs

Two programs which permit filtering of data in either the frequency domain or time domain were written. One filtering program permits magnification of data about the center of a square or rectangular array of transformed measured data. A second program permits location of the "magnified" region anywhere within the measured data array. By filtering the transformed data, any specific region of interest of a scanned target can be magnified and the resolution in that particular region increased. This is accomplished by making all data points in the transformed data array (from the original total measured data array) outside a specific sub-region equal to zero. Upon performing an inverse Fourier transform of the filtered data, the resolution of the region of interest is expanded to fill an array which is the same size as the original total measured data array. This algorithm was written during this pilot study, but it has not been tested.

SECTION VI
EXPERIMENTAL INVESTIGATIONS

One of the primary objectives of this pilot research effort was to examine the feasibility of imaging structures embedded in lossy dielectric materials (i.e., organs or other structures within a biological target). During this program, we conducted a limited number of feasibility studies using dielectric-loaded antennas in conjunction with a simple electromechanical scanner. These studies have shown that dielectric structures in tissue-equivalent phantom models (pliable models having electromagnetic properties of actual tissues) have been imaged at several centimeters depth. At the Walter Reed Army Institute of Research, feasibility studies have been conducted using a microwave system at 3.9 GHz to image phantom targets and isolated canine kidneys [3,4]. Their system included electromechanical scanning and computer-aided processing techniques. No tomographic reconstruction was done. Their published results revealed an unprocessed image resolution of approximately 6 mm.

These results have been confirmed in feasibility studies conducted in our laboratory (under Project B-508). A block diagram of the instrumentation setup used is given in Figure 7. In our studies, the target consisted of an approximately 15 cm by 15 cm Plexiglas box, 6-cm thick, which was filled with tissue-equivalent phantom material. The target was placed between two opposing dielectric-loaded antennas oriented along a common axis. Midway in the thickness of the target was embedded a dielectric rod 3 mm in diameter and approximately 12 cm in length oriented parallel to the linear polarization of the two antennas. The two antennas, aligned on-axis, were raster-scanned in the X-Y plane, with each X-cut recorded on an X-Y plotter. Raw, unprocessed transmitted phase data for azimuthal scans with and without the rod present are shown in Figure 8. The forward scattered field due to the dielectric rod alone is shown in Figure 9, which is the difference between the total field with the rod present and with the rod absent. Our results for these simple tests are similar to those obtained in the study conducted by Larsen and Jacobi [3], except that the ability to resolve the dielectric rod in our intial studies was better (3-mm dia. rod vs. 6-mm dia. rod). Measured transmitted phase results for two 3-mm diameter rods spaced 11 mm apart

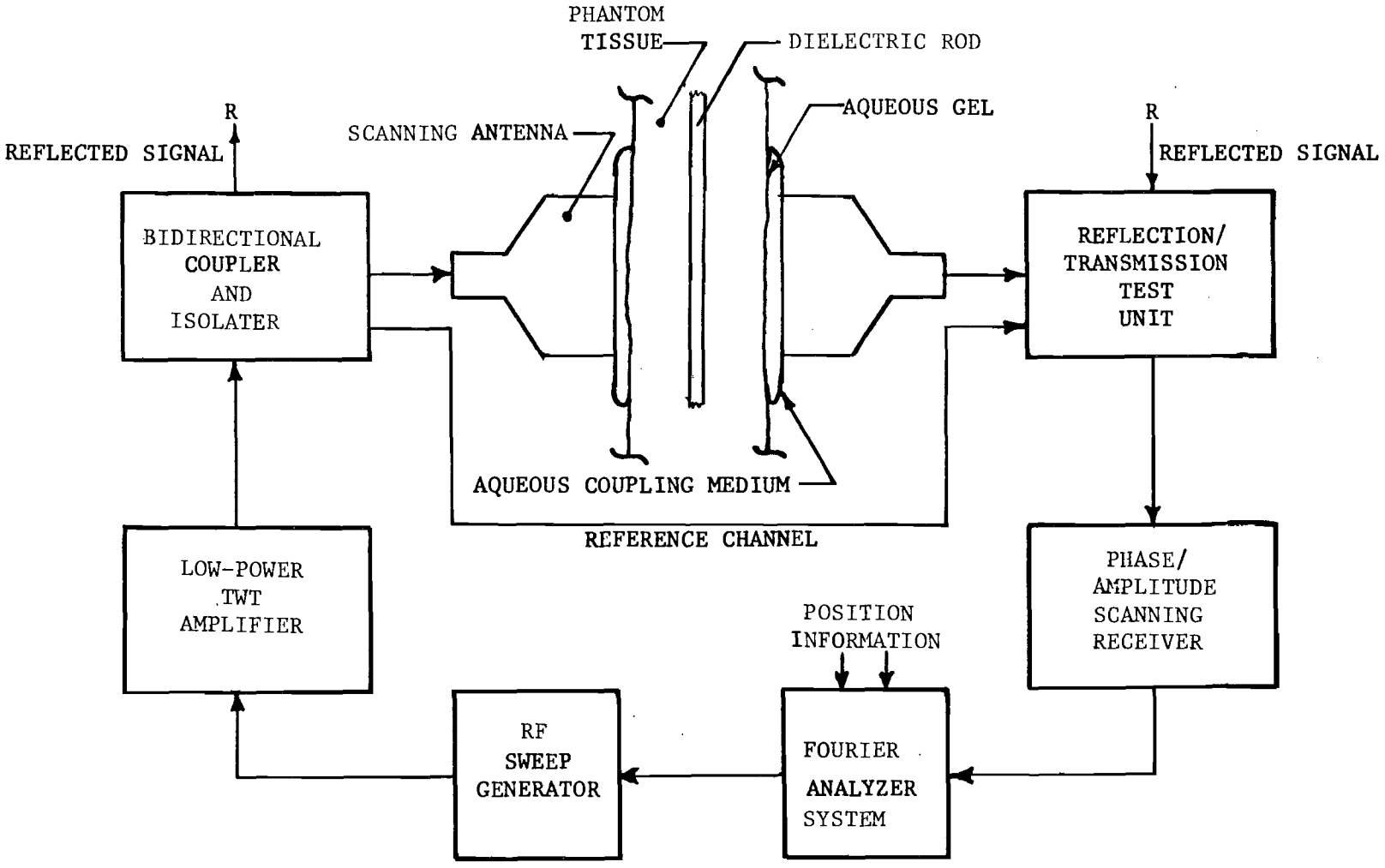

Figure 7. Block Diagram of a Scattering Parameter Microwave Imaging System. Computer data acquisition and processing system are included in Fourier Analyzer System.

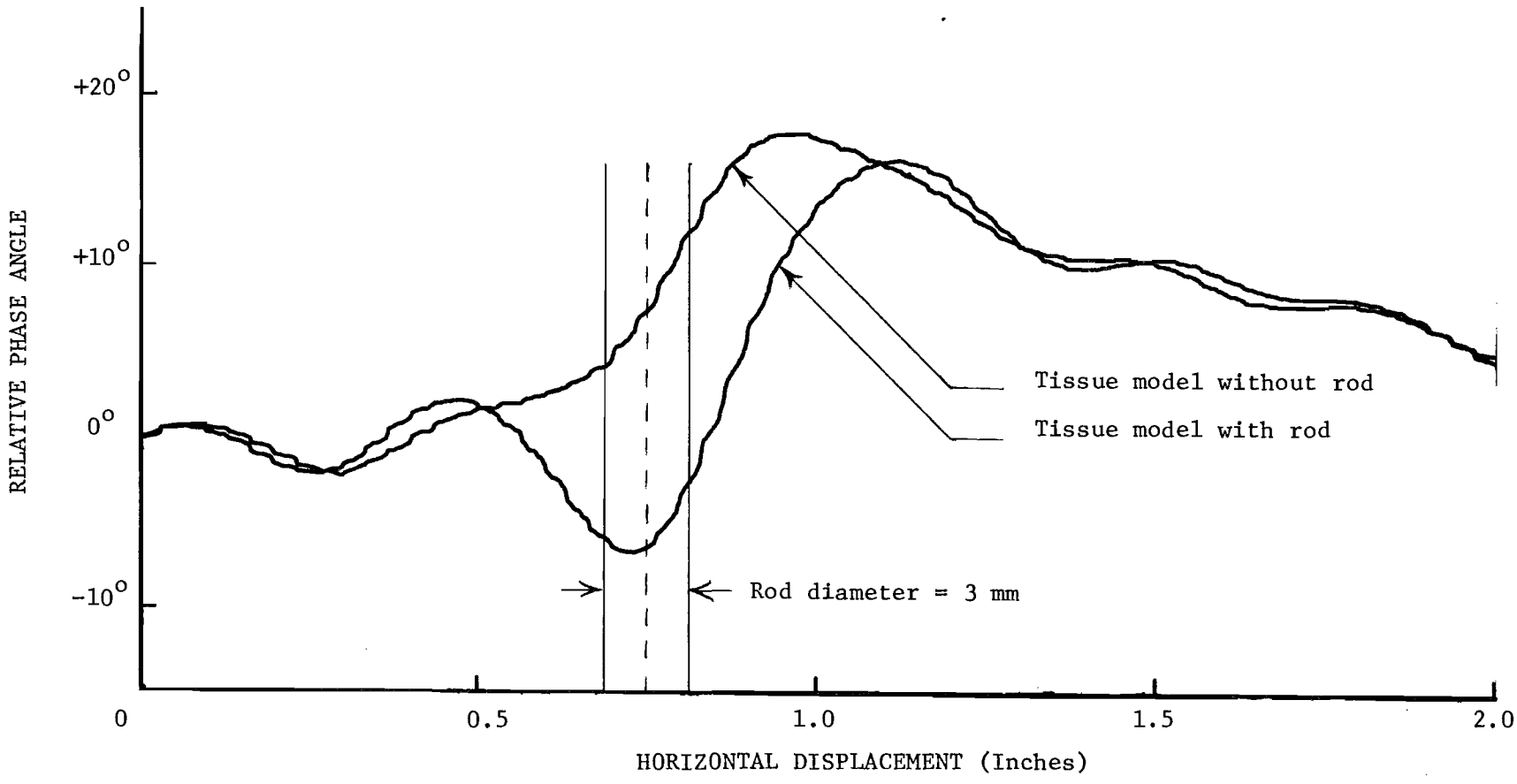

Figure 8. Phase variation of 3 GHz transmitted wave in tissue phantom model with one 3-mm diameter dielectric rod located midway between transmitting and receiving antennas.

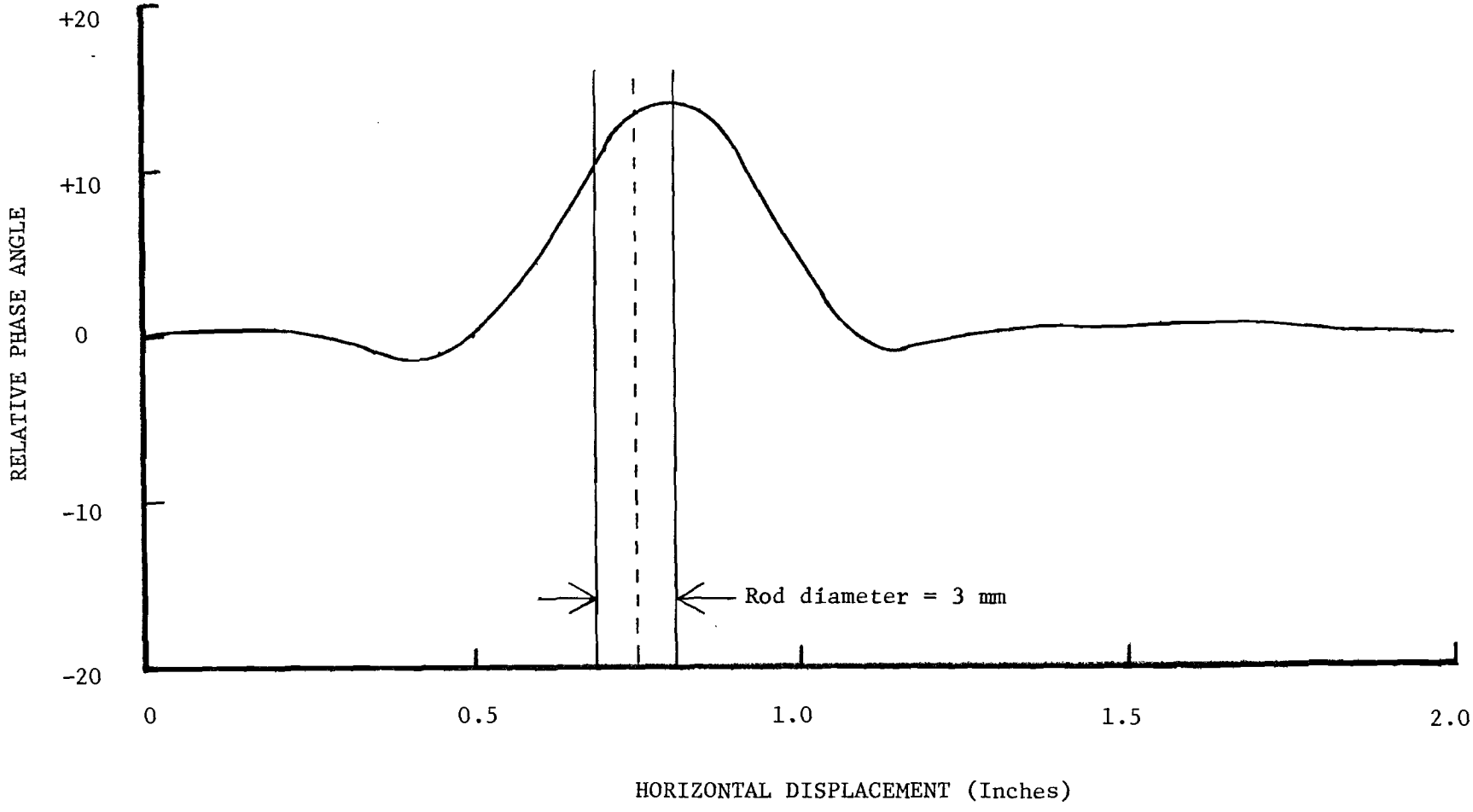

Figure 9. Difference between measured phase variation of 3 GHz transmitted wave in tissue phantom model without target and with one 3-mm diameter dielectric rod located midway between transmitting and receiving antennas.

are presented in Figure 10 and the difference pattern is shown in Figure 11. No data processing was done to improve image quality in any of these feasibility tests. From these data, it is apparent that it is possible to discriminate between rods located one-third the separation distance (or 4 mm). For this case, discrimination is essentially equivalent to resolution. (In the strict sense, however, resolution is the ability to separate two or more scatterers, while discrimination is the ability to discern between tissues of differing dielectric properties. In biological systems, these quantities are often in effect the same). Again, our results are a factor of two better than those obtained in a similar study for those cases where no signal processing was employed [3]. This improvement in "raw data resolution" is attributed largely to the difference in antennas used in the different feasibility studies. Figures 12-15 show similar results for cases identical to those depicted in Figures 8-11 except that the measured parameter was the magnitude of the transmitted signal, rather than the phase. In examining these results (Figures 8-15), it is noteworthy that while system sensitivity per se is not a determiner of resolution, the ability to resolve the diameter of each of the rods is related to the measured signal-to-noise ratio. Figure 16 displays a two-dimensional image of measured phase data for the case of Figure 11, except that horizontal scans were made for multiple vertical positions to form the image. A FFT and an inverse transformation using the Bivariate interpolation program were used to process the two-dimensional image.

In the studies involving microwave imagery of isolated canine kidneys [3,4], magnitude and phase transmission data were sufficient to reveal information which could be related to structural organization within the kidney. Unlike phantom model studies, however, these data were processed and displayed by either monochrome or pseudocolor maps. This processing consisted of data truncation, followed by cubic-spline interpolation, to increase the digital data base from a 64 x 64 array to a 256 x 256 array. The two-dimensional power spectrum was computed to determine the maximum spatial frequency present in the kidney data. Using this information, a two-dimensional bandpass filter was selected and used to digitally filter the magnified data. The filtered data were then displayed as stated above. Regions corresponding to filtration were separable from regions corresponding to osmotic concentration, and both were easily separable from the pelvis. It is evident that this relatively straightforward data processing results in an improvement in resolution with respect to that obtainable from raw, unprocessed data.

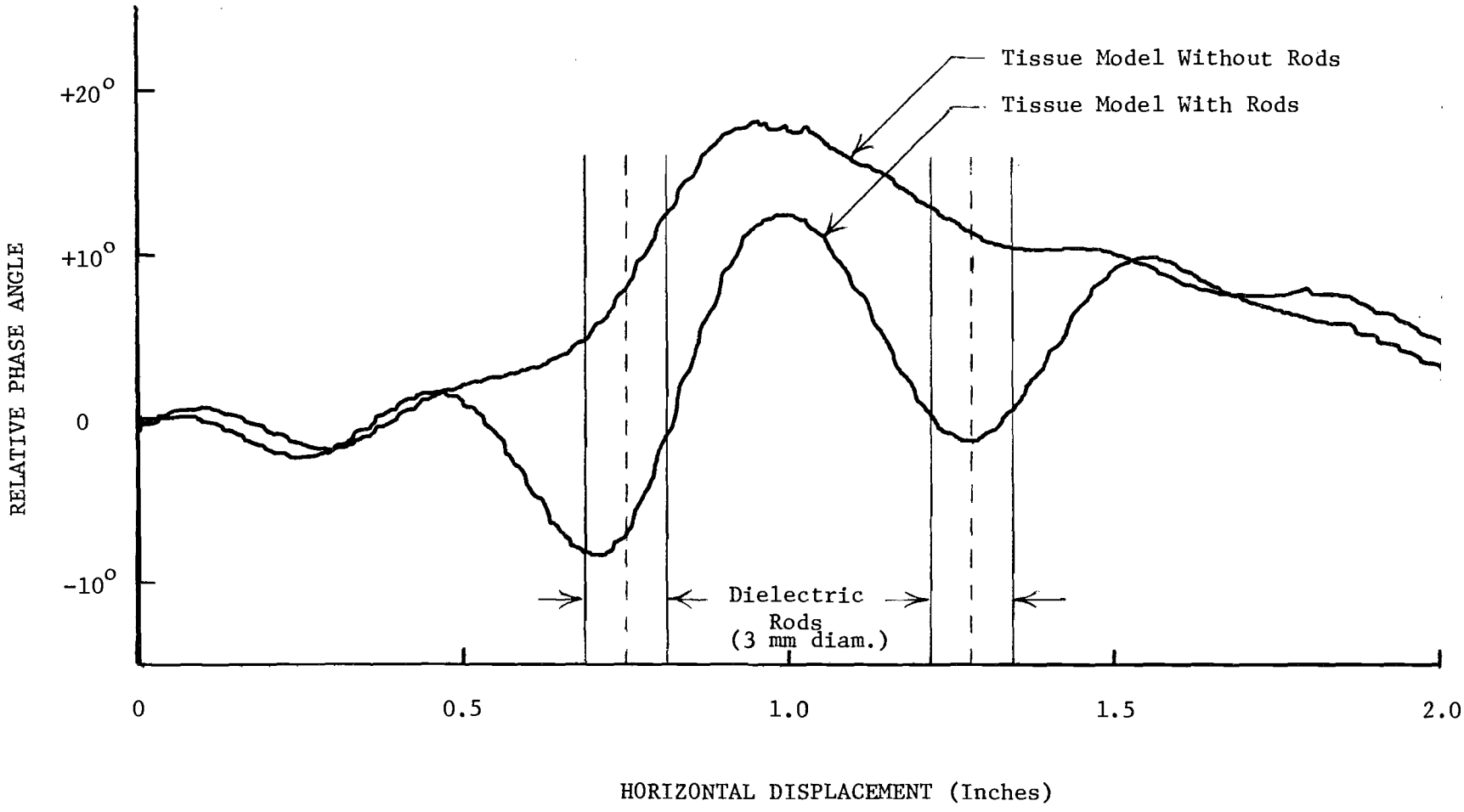

Figure 10. Phase variation of 3 GHz transmitted wave in tissue phantom model with two 3-mm diameter dielectric rods spaced 11 mm apart and located midway between transmitting and receiving antennas.

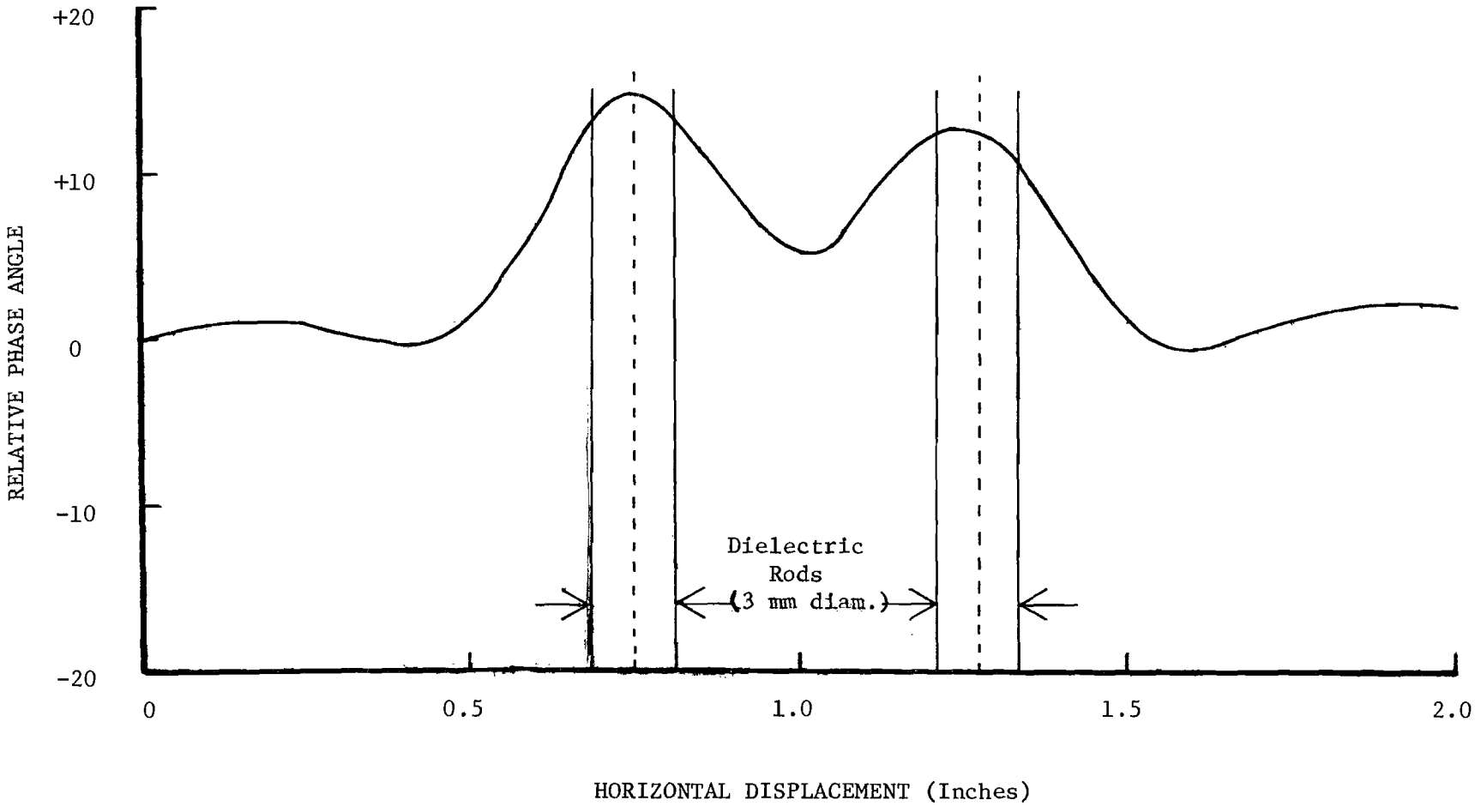

Figure 11. Difference between measured phase variation of 3 GHz transmitted wave in tissue phantom model without target and with two 3-mm diameter dielectric rods spaced 11 mm apart and located midway between transmitting and receiving antennas.

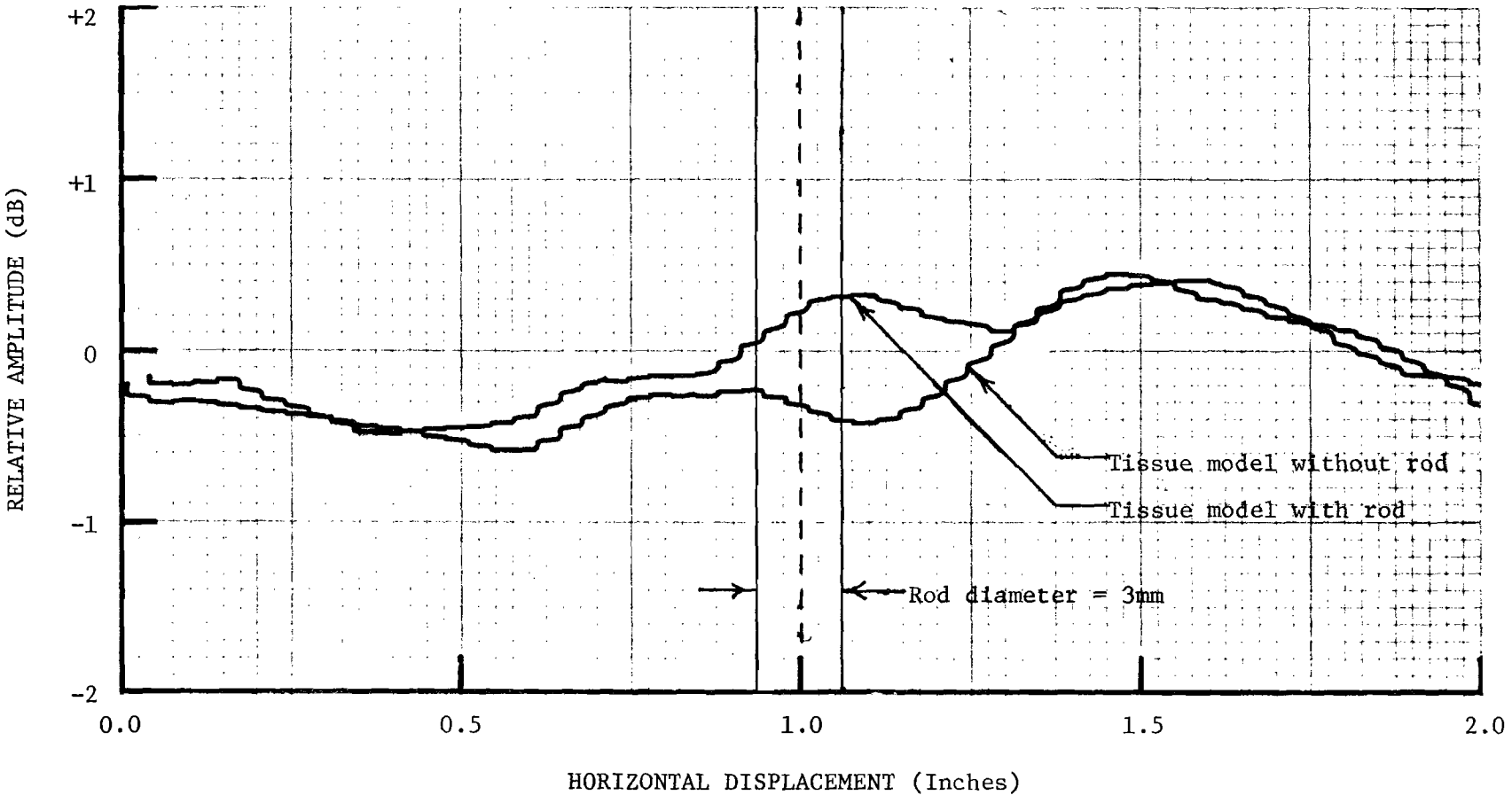

Figure 12. Amplitude variation of 3 GHz transmitted wave in tissue phantom model with one 3-mm diameter dielectric rod located midway between transmitting and receiving antennas.

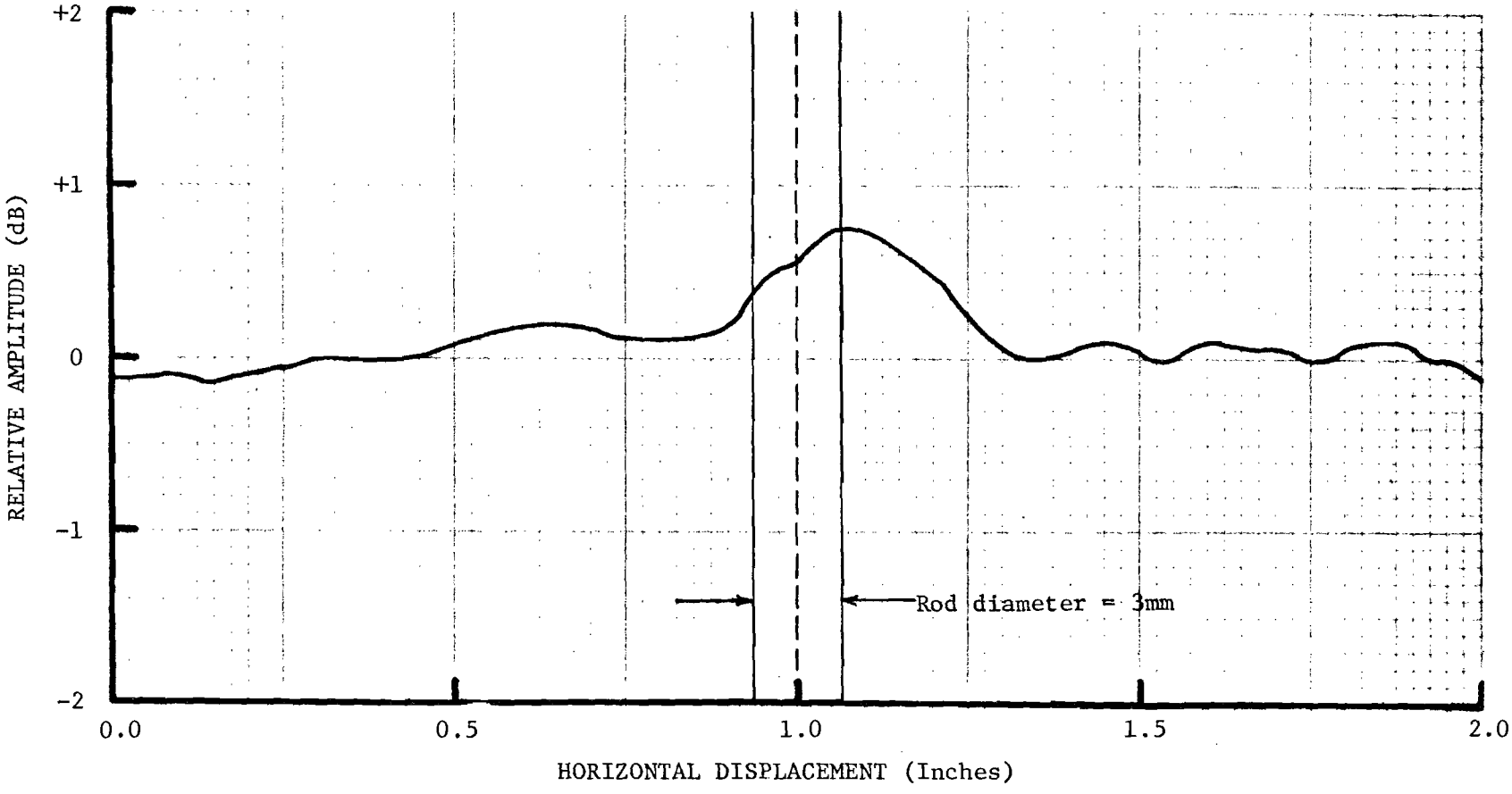

Figure 13. Difference between measured amplitude variation of 3 GHz transmitted wave in tissue phantom model without target and with one 3-mm diameter dielectric rod located midway between transmitting and receiving antennas.

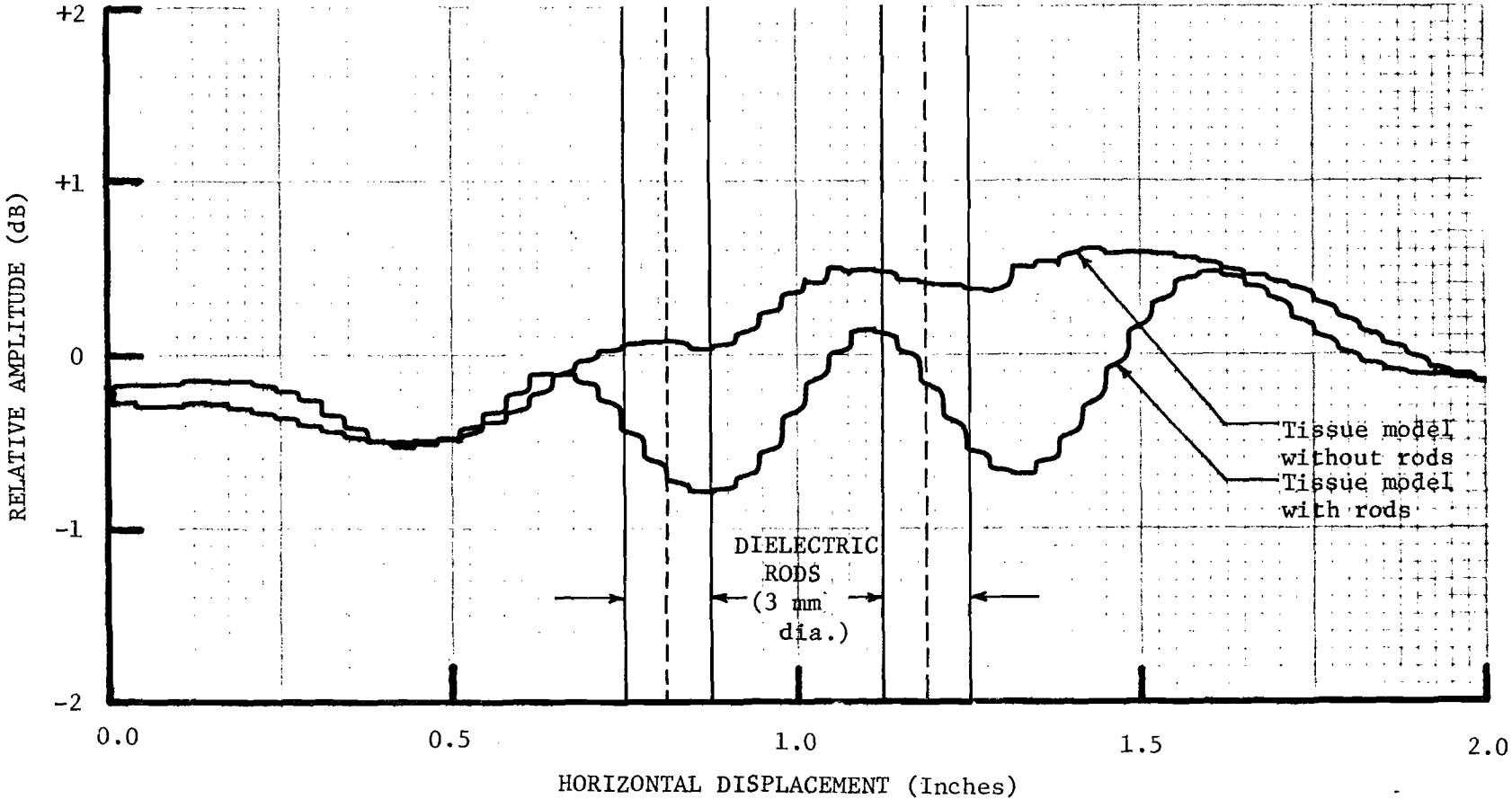

Figure 14. Amplitude variation of 3 GHz transmitted wave in tissue phantom model with two 3-mm diameter dielectric rods spaced 13 mm apart and located midway between transmitting and receiving antennas.

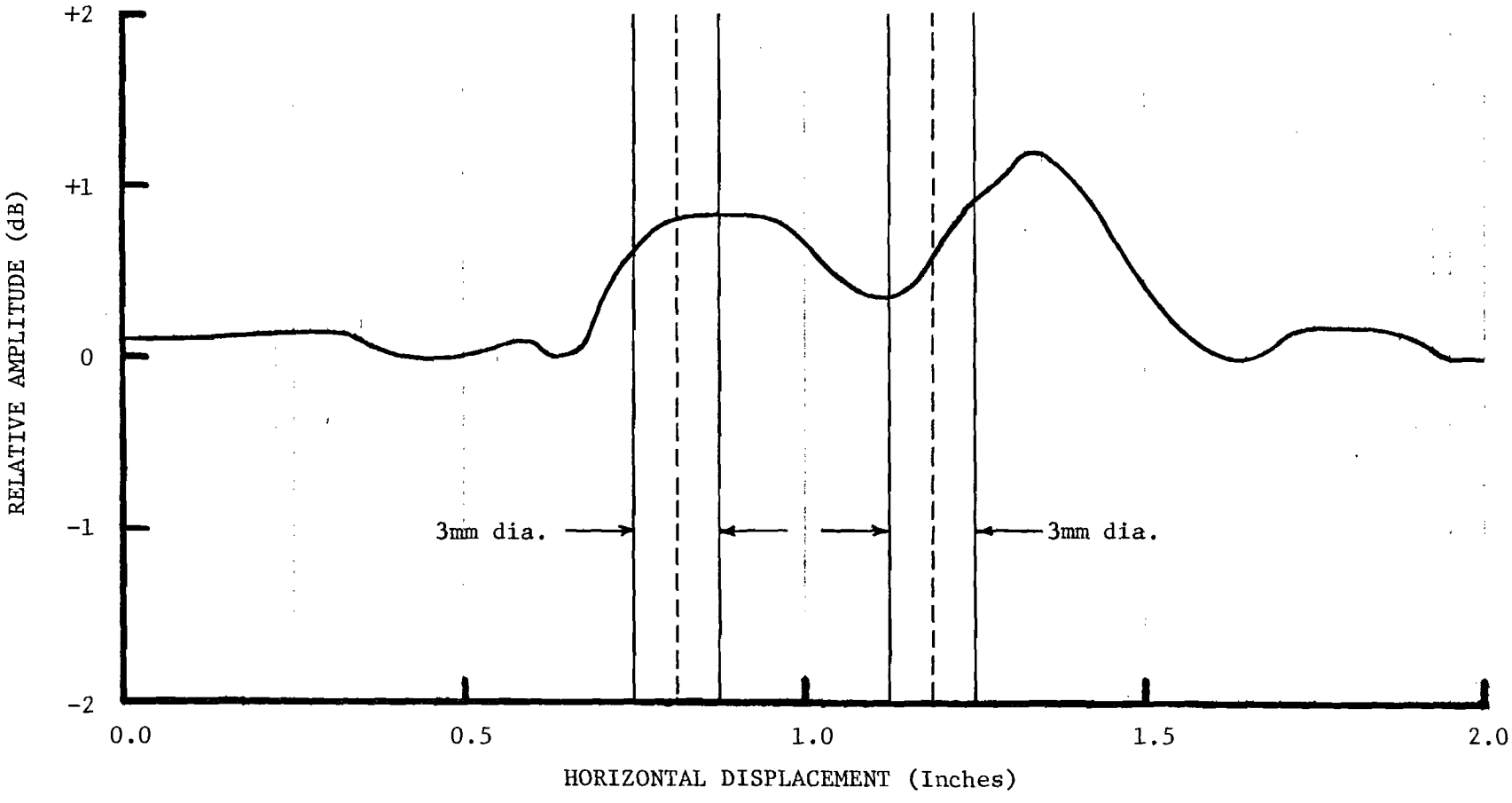

Figure 15. Difference between measured amplitude variation of 3 GHz transmitted wave in tissue phantom model without target and with two 3-mm diameter dielectric rods spaced 13 mm apart and located midway between transmitting and receiving antennas.

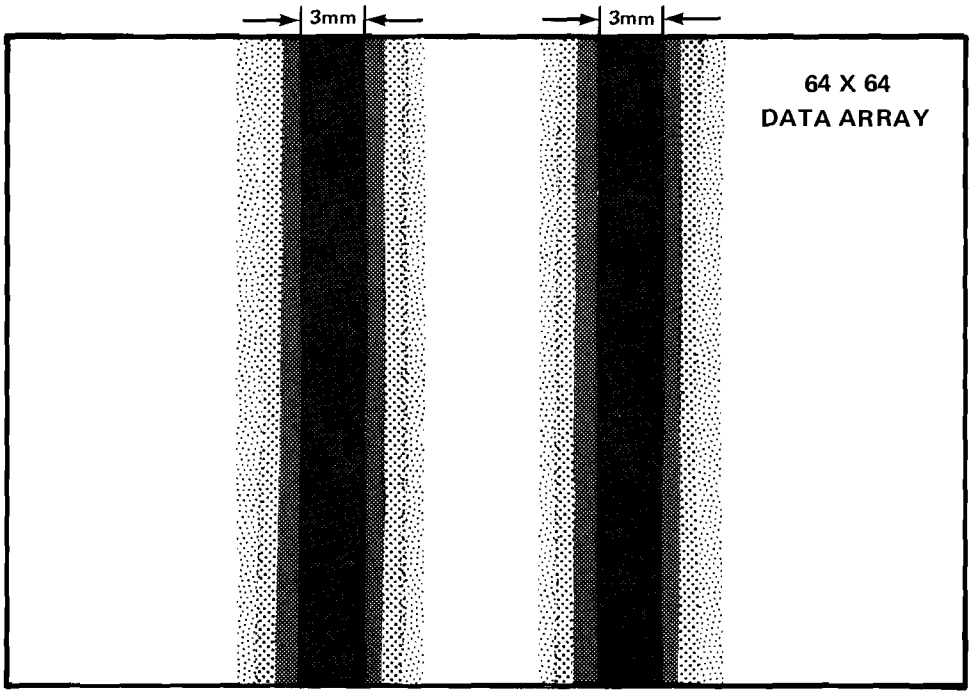

(a)

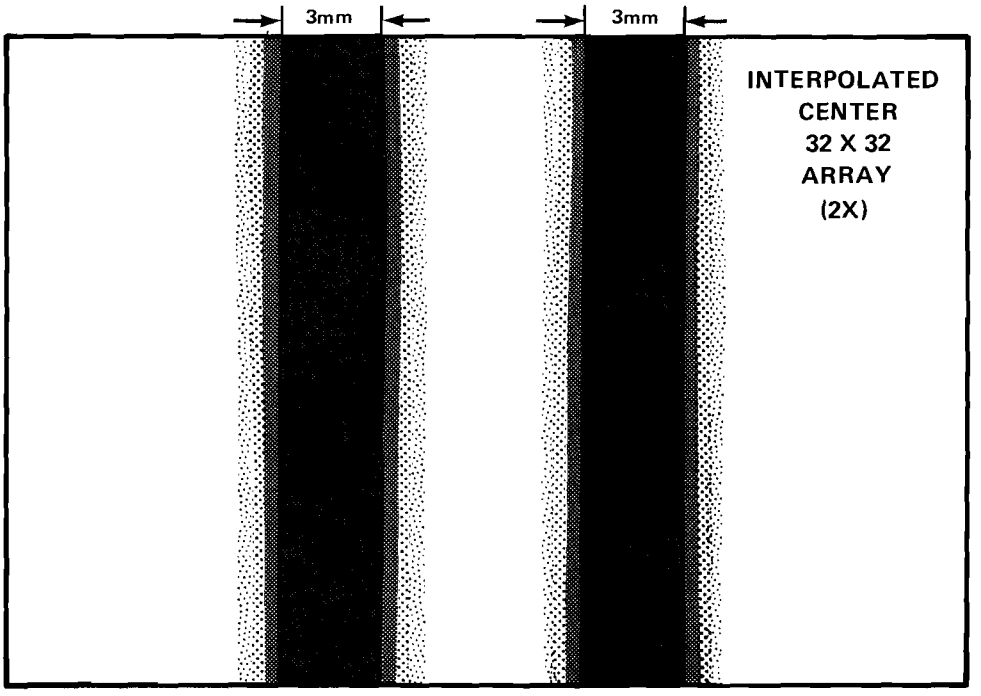

(b)

Figure 16. Two-dimensional plot of measured phase variation of 3 GHz transmitted signal through tissue phantom model with two 3-mm diameter dielectric rods spaced 11 mm apart and located in phantom model midway between transmitting and receiving antennas. (a) Unprocessed data, (b) transformed and interpolated data with interpolation window centered midway between the dielectric rods.

SECTION VII
CONCLUSIONS

The development of a non-invasive imaging technique based on the use of non-ionizing EM energy offers potential for satisfying many of the criteria of "ideal" diagnostic imaging instrumentation listed on pages 1 and 2 (Section I). In addition to imaging anatomical structures, with the use of non-ionizing energy in the UHF/microwave portion of the EM spectrum it may well be possible also to assess functional status based on physiologically-relevant information contained in the received EM signal. This unique potential exists because of the biological relevance of complex permittivity (dielectric properties) to physiological function. Recent research [19,20] indicates that changes in bulk flow and hydration state of water in a functioning biological system are reflected by changes in the local/regional dielectric properties of that system.

The overall objective of this effort was to evaluate the feasibility of using microwave imaging techniques as a means for non-invasive interrogation of biological systems. The interaction of parameters which affect the achieveable resolution and penetration were assessed, and from that assessment general guidelines for selection of operating frequency range, power level(s), antenna design, receiver sensitivity and noise limitations, and data processing were established. The general conclusions of that assessment are that (1) the most practical frequency range for operation would be 2-6 GHz (based on penetration/resolution tradeoffs), (2) required incident power density would vary depending upon specific operating frequency but must not exceed 0.5 mW/cm^2 and must be at least 0.01 mW/cm^2 (@ 3 GHz) for use with the best available state-of-the-art microwave phase-amplitude receiver, (3) impedance matching between the antenna(s) and the biological target is crucial to detection sensitivity, (4) small-aperture multi-element antennas would likely perform better than larger single-element antennas, (5) scanner antenna positioning accuracy and repeatability are crucial to ultimate image resolution/processing, (6) a very low noise figure receiver and high-gain preamplifier are required if low incident transmitted power levels are to be used, and (7) structures with a large dielectric discontinuity at the

internal interface of interest can be imaged with little or no data processing (Figures 8-16), but the detection of subtle dielectric changes due to physiological/patho-physiological influences requires the use of sophisticated digital data processing methods. The work performed under this pilot study demonstrated that the detection and imaging of internal structures in lossy dielectric targets (muscle-equivalent phantoms) is possible even with only minimal data processing. Only limited testing of the data processing software developed was performed. Application of the Fourier transform and Bivariate Interpolation routines for filtering existing raw experimental data resulted in a "cleaner" image because of the interpolation of additional points. However, the total data matrix size is limited by the maximum allowable data block size and computer storage. Also, regions of greater interest can be enlarged or "blown up" through judicious bandpass filtering. With further significant development efforts, detection and imaging of small dielectric anomalies in biological targets should be achieveable.

SECTION VIII
REFERENCES

1. L.E. Larsen, and J.H. Jacobi, "Microwave Interrogation of Dielectric Targets. Part I: By Scattering Parameters", Med. Phys. 5:500-508, 1978.

2. J.H. Jacobi and L.E. Larsen, "Microwave Interrogation of Dielectric Targets. Part III: By Microwave Time Delay Spectroscopy", Med. Phys., 5:509-513, 1978.

3. L.E. Larsen and J.H. Jacobi, "Microwave Scattering Parameter Imagery of an Isolated Canine Kidney", Med. Phys., 6:394-404, 1979.

4. J.H. Jacobi and L.E. Larsen, "Microwave Time Delay Spectroscopic Imagery of Isolated Canine Kidney", Med. Phys. Vol 7:1-7, 1980.

5. R.K. Lambert and H. Gremels, "On the Factors Concerned in the Production of Pulmonary Edema", J. Physiol. (London), Vol. 61:98-112, 1926.

6. A. Kolin, "Electromagnetic Flowmeter: Principle of Method and Its Application to Blood Flow Measurements", Proc. Soc. Exp. Biol. Med., Vol. 35:53-56, 1936.

7. C. Cappelin, Jr. and K.V. Hall, "Electromagnetic Blood Flowmetry in Clinical Surgery", Acta. Chiv. Scand., Suppl. 368, pp.3-37, 1967.

8. B.T. Williams, et al., "Continuous Long-term Measurement of Cardiac Output After Open Heart Surgery", Ann. Surg., Vol. 174, pp. 357-363, 1971.

9. C. Susskind, "Possible Use of Microwave in the Management of Lung Disease", Proc. IEEE (Letters), 61:673, 1973.

10. P.C. Pedersen, et al., "Microwave Reflection and Transmission Measurements for Pulmonary Diagnosis and Monitoring", IEEE Trans. Biomed. Engr., BME-25:40-48, 1978.

11. S.S. Stuchly, et al., "Monitoring of Arterial Wall Movement by Microwave Doppler Radar", presented at the Symp. EM Fields in Biol. Sys., Ottawa, Ont. Canada, June 27-30, 1978.

12. J.C. Lin, "Noninvasive Microwave Measurement of Respiration", Proc. IEEE (Letters), 63:1530, 1975.

13. I. Yamamura, "Measurement of Heart Dynamics Using Microwaves - Microwave Stethoscope", Inst. Electron. Commun. Eng. Japan, Vol. TG-EMC-J78-15, pp. 9-14, 1978.

14. E.C. Burdette and J. Seals, "A Technique for Determining the Electrical Properties of Living Tissues at VHF Through Microwave Frequencies", Proc. of the 1977 IEEE Region 3 Conference and Exhibit, Williamsburg, VA, April 1977.

15. E.C. Burdette, F.L. Cain, and J. Seals, "In-Vivo Determination of Energy Absorption in Biological Tissue," Final Technical Report, Project A-1755, U.S. Army Research Office Grant No. DAAG29-75-G-0182, January 1979.

16. E.C. Burdette, F.L. Cain, and J. Seals, "In-Vivo Probe Measurement Technique for Determining Dielectric Properties at VHF Through Microwave Frequencies", IEEE Trans. Microwave Theory Tech., MTT-28:414-428, 1980.

17. E.C. Burdette, R.L. Seaman, J. Seals, and F.L. Cain, "In-Vivo Techniques for Measuring Electrical Properties of Tissues", Annual Technical Report No. 1, Project A-2171, U.S. Army Medical Research and Development Command, Contract No. DAMD17-78-C-8044, July 1979.

18. E.C. Burdette, F.L. Cain, and J. Seals, "In-Situ Permittivity Measurements: Perspective Techniques, Results," Electromagnetic Dosimetric Imagery Symposium, 1980 IEEE MTT-S International Symposium, Washington, D.C., May 1980 (IEEE Press, New York).

19. E.C. Burdette, P.G. Friederich, R.L. Seaman, and V.P. Popovic, "Postmortem Changes in Canine Brain Permittivity Measured In-Situ", Abstracts of the Third Annual Conference of the Bioelectromagnetics Society, Washington, D.C., August 1981.

20. E.C. Burdette, S.R. Crowgey, P.G. Friederich, and V.P. Popovic, "Renal Physiological Changes Determined from Tissue Impedance Measurements" Abstracts of the Fourth Annual Scientific Session of the Bioelectromagnetics Society, Los Angeles, CA., June 28-July 2, 1982.

21. E.C. Burdette, J. Seals, R.L. Magin, and S.P. Auda, "A-Priori Determination of Power Absorption in Hyperthermia Based on In-Vivo Dielectric Measurements", Proc. of the Third Intern'l Symposium: Cancer Therapy by Hyperthermia, Drugs, and Radiation, Fort Collins, CO., June 1980.

22. J. Seals and E.C. Burdette, "Comparison of Dielectric Properties of In-Vivo Rat Brain, Muscle, and Tumor," Digest of the 1981 Microwave Power Symposium, 176-178, Toronto, June 1981.

23. E.C. Burdette, "Electromagnetic and Acoustic Properties of Tissues", in PHYSICAL ASPECTS OF HYPERTHERMIA, Ed.: G.H. Nussbaum, and presented at the AAPM Summer School, Dartmouth College, Hanover, NH, August 1981.

24. J.H. Jacobi, L.E. Larsen, and C.T. Hast, "Water-immersed Microwave Antennas and Their Application to Microwave Interrogation of Biological Targets", IEEE Trans. Microwave Theory Tech., MTT-27, No. 1, 70-78, Jan. 1979.

25. H.G. Schmidt-Weinmar, "Spatial resolution of subwavelength sources from optical far-zone data", Inverse Source Problems in Optics, Editor: H.P. Baltes, Springer-Verlag, New York, 1978, pp. 83-116.

26. B.J. Hoenders, "The uniqueness of inverse problems", Inverse Source Problems in Optics, Editor: H.P. Baltes, Springer-Verlag, New York, 1978, pp. 41-82.

27. M.B. Katz, "Questions of uniqueness and resolution in reconstruction from projections", Lecture Notes in Biomathematics, Vol. 28, Springer-Verlag, New York, 1978.

28. B. Enander and G. Larson, "Microwave radiometric measurements of the temperature inside a body", Electronics Letters, Vol. 10, No. 15, 25 July 1974.

29. A.H. Barrett and P.C. Myers, "Microwave thermography: Noninvasive sensing of subcutaneous temperatures", Proc. International Symp. on Cancer Therapy by Hyperthermia and Radiation, Washington, D.C., April 1975.

30. P.C. Myers, et al., "Microwave thermography: Principles, Methods and Clinical Applications", J. Microwave Power, Vol. 14, No. 2, pp. 105-115, 1979.

31. A.H. Barrett and P.C. Myers, "Subcutaneous temperatures: A method of noninvasive sensing", Science, Vol. 190, 14 Nov. 1975.

32. A.H. Barrett, et al., "Microwave Thermography: Application to the Detection of Breast Cancer", in Prevention and Detection of Cancer, H.E. Nieburgs, ed. Marcel Dekker, Inc., 1978.

33. J. Edrich, "Centimeter - and Millimeter-wave Thermography - A Survey of Tumor Detection", J. Microwave Power, Vol. 14, No. 2, pp. 95-104, 1979.

34. I. Yamaura, "Measurements of 1.8 - 2.7 GHz Microwave Attenuation in the Human Torso", IEEE Trans. Microwave Theory Tech. MTT-25, 707 (1977).

35. H.P. Schwan, "Electrical properties of tissue and cell suspensions", Advan. Biol. Med. Phys., Vol. 5, pp. 147-209, 1957.

36. L.E. Larsen, J.H. Jacobi, and A.K. Krey, "Preliminary Observations with an Electromagnetic Method for the Non-invasive Analysis of Cell Suspension Physiology and Induced Pathophysiology, IEEE Trans. Microwave Theory Tech., MTT-26, 581-595, 1978.

37. W.T. Joines, Eiji Tanabe, and Raymond U., "Determining the electrical properties of normal and malignant biological tissue in-vivo", Proceedings of 1976 IEEE Southeastern Conference and Exhibit, Clemson, SC, 1976.

38. H.P. Schwan and K.R. Foster, "RF-field interactions with biological systems: electrical properties and biophysical mechanisms", Proc. IEEE, Vol. 68, No. 1, p. 104-113, 1980.

39. E.H. Grant, S.E. Keefe, and S. Takashima, "The dielectric behavior of aqueous solutions of bovine serum albumin from radiowave to microwave frequencies", J. Phys. Chem., Vol. 72, p. 4373-4380, 1968.

40. S. Ramo, J.R. Whinnery, T. Van Duzer, Fields and Waves in Communication Electronics, John Wiley, New York, 1965.

41. R. Pethig, Dielectric and Electrical Properties of Biological Materials, John Wiley, New York, 1979.

42. M. Born and E. Wolf, Principles of Optics, Pergamon Press, New York, 1959, pp. 332-333.

43. M. Abramowitz and I.A. Stegun, Handbook of Mathematical Functions, National Bureau of Standards, Applied Mathematics Series - 55, 1964.